Power Systems Engineering Research Center

ACCURACY IMPROVEMENT STRATEGIES FOR PROBLEMATIC POWER SYSTEM MEASUREMENTS AND THEIR EFFECT ON STATE ESTIMATION

A Supplementary Project Report for Project S-22

Brian C. Mann
G. T. Heydt
Arizona State University

PSERC Publication 06-XX

July 2006

Information about this project

For information about this project contact:

Gerald T. Heydt, Ph.D.
Arizona State University
Department of Electrical Engineering
Tempe, AZ 85287
Tel: 480-965-8307
Fax: 480-965-0745
Email: heydt@asu.edu

Power Systems Engineering Research Center

This is a project report from the Power Systems Engineering Research Center (PSERC). PSERC is a multi-university Center conducting research on challenges facing a restructuring electric power industry and educating the next generation of power engineers. More information about PSERC can be found at the Center's website: http://www.pserc.org.

For additional information, contact:

Power Systems Engineering Research Center

Arizona State University

P. O. Box 875706

Tempe, AZ 85287-5706

Notice Concerning Copyright Material

Executive Summary

This research discuses several power system measurement pre-processing techniques, which may improve calculations like state estimation (SE). SE is a proven technology, but operates under assumptions which may be inappropriate. The concept of non-collocated power measurement error is introduced, where reactance between current and voltage instruments creates power calculation error. A calculation-based method for correcting these measurements is presented and shown to slightly improve state estimates. SE may assume balanced operation. However, unbalance is common in power systems. Under certain assumptions, single-phase power measurements and complex current unbalance factor (CCUF) can calculate three-phase power. This yields better measurements, but is shown to have little effect improving traditional SE. Methods for estimating or calculating CCUF are also presented. SE often assumes all measurements are simultaneous. A simple linear prediction method used to identify late measurements is studied and shown to work in systems with low measurement noise and low system dynamics.

The main elements of this research are:

- It is possible to correct the measurement error associated with reactance in-between the CT and PT component of a power measurement from knowing the non-collocated power measurement, a local voltage magnitude, and the reactance. This is a software solution that avoids hardware reinstallation and may have a positive effect of state estimation results by lowering estimate error and, more

dramatically, lowering state estimate variance. The practical significance of this is that a software patch can be used to correct for non-collocated power measurements, thereby avoiding a hardware fix.

- State estimators that incorporate three-phase power flow may operate under a balanced system assumption when unbalanced conditions. A more accurate three-phase power calculation may be calculated from single-phase measurements and the complex current unbalance factor, resulting in improved state estimation output. Methods for estimating or directly calculating the complex current unbalance factor are also presented. The practical significance of this is that through a software correction procedure, at least under some circumstances, it may be possible to correct for unbalanced measurements.

- A linear signal prediction algorithm is presented which may have a positive effect on power system state estimation in the presence of measurement latency. The presented algorithm has the advantage of being less complex than existing delayed measurement correcting algorithms presented in the literature. The value of this technical topic is that latency can be compensated through a software patch, and at least three methods are described in this report.

ACKNOWLEDGEMENTS

The authors thank the generous support of the Power Systems Engineering Research Center, and the support of the Salt River Project (SRP) for this project. In particular, the following investigators at SRP are acknowledged for their support and expertise: G. Strickler, N. Logic, S. Sturgill, J. Singh.

The authors also thank Dr. Daniel J. Tylavsky and Dr. Vijay Vittal for their technical input. The authors acknowledge the technical contributions of Ms. Lida Jauregui – Rivera. Thanks is also due for Professor Richard G. Farmer, whose valuable experience and helpfulness played a role in the first part of this research. Useful comments of L. Jerriel were used in the project and we acknowledge Mr. Jerriel's input.

TABLE OF CONTENTS

Page

Page

TABLE OF FIGURES

Page

TABLE OF TABLES

Page

Page

NOMENCLATURE

a	A complex phasor $1\angle -120°$ and a real number which is a magnitude of a bus voltage V_1
A	Matrix that linearly relates past measurements to future measurements
AC	Alternating current
A/D	Analog/digital
ARMA	Mixed auto-regressive moving average
b	A variable which is the real component of the current through line reactance X_1
c	A variable which is the imaginary component of a current through line reactance X_1
CT	Current transformer
CUF	Current unbalance factor
d	A variable which is the real component of a mid-line voltage V_x
δ_a	Voltage phase angle of bus a
e	A variable which is the imaginary component of a mid-line voltage V_x
EMS	Energy management systems
f	A variable which is the real component of a current through line reactance X_2
g	A variable which is the imaginary component of a current through line reactance X_2
GPS	Global positioning system
h	A variable which is the real voltage of a bus voltage V_2
H	State estimation coefficient matrix
i	Counter index
I_+	Positive sequence current
I_-	Negative sequence current
I_0	Zero sequence current
I_{ab}	Current between buses a and b
$I_{a,\,b,\,c}$	Current for phase a, b, or c
IEEE	Institute of Electrical and Electronics Engineers
j	Complex number $\sqrt{-1}$
$J(x)$	Jacobian matrix
k	A variable which is the imaginary component of bun voltage V_2 or a time step variable in the discrete Kalman filter algorithm
K	The Kalman gain, in the discrete Kalman filter
M	Measurement-to-branch matrix and symmetrical component transformation index
N_m	Number of measurements
N_s	Number of states
P	Active power and the error covariance matrix in the discrete Kalman filter
PMU	Phasor measurement unit
PT	Potential transformer
p.u.	Per-unit

Q	Reactive power and the expected value of noise w^2 in the discrete Kalman filter
R	Covariance matrix of measurement errors, weighting matrix
S	Complex power
$S_{3\varphi}$	Three-phase complex power
S_{ab}	Complex power calculated from V_a and I_b
SE	State estimation
t	Time in seconds
U_I	Current unbalance factor
U_V	Voltage unbalance factor
UTC	Coordinated Universal Time
v	Measurement error in discrete Kalman filter algorithm
V	Voltage (rms phasor)
$V_{1+,\ 2+}$	Positive sequence voltage for bus 1 or 2
V_+	Positive sequence voltage
V_-	Negative sequence voltage
V_0	Zero sequence voltage
$V_{a,\ b,\ c}$	Voltage for phase *a, b*, or *c*
$\lvert V\rvert_a$	Voltage magnitude of bus *a* or point *a*
VUF	Voltage unbalance factor
w	White noise associated with a measurement
W	Residual sensitivity matrix
WLS	Weighted least squares
x	Vector of state values
X	Reactance
z	Vector of measurements
η	Measurement error
φ	Matrix which relates x_k to x_{k+1} in the discrete Kalman Filter

CHAPTER 1 STATE ESTIMATION

1.1 State estimation: an introduction

State estimation (SE) is a mathematical process in which physical measurements and physical models are combined in an optimal way. That is, measurements taken in the field are used with models and the states of the system (in the power engineering application, the states are typically the bus voltage phase angles and magnitudes) are selected or calculated such that the states match the measurements in some best way. The usual SE technique utilizes what is known as the least squareserror algorithm. In this algorithm, the system model is linearized as

$$z = Hx,$$

where z is a vector of measurements, x is the system states (a vector), and H is the relationship between the measurements and the states. The matrix H is also known as the process matrix. If z is an m-vector, and x is an n-vector, then H is an m by n rectangular matrix. Typically,

$$m >> n.$$

The SE process is the minimization of $|Hx - z|$. In the least squares algorithm, the norm indicated is a Euclidean norm. In essence, the SE algorithm causes x to be selected such that $|Hx - z|$ is minimized. The notation $\hat{x}$ (read 'x – hat') is the estimate of the state vector x at this minimum. The vector

$$H\hat{x} - z = R$$

is called the residual vector, and the Euclidean norm,

$$|H\hat{x} - z|_2 = r$$

is the residual magnitude.

The SE solution involves taking the pseudoinverse of the process matrix H denoted as H^+. The optimal x, that is the best estimate of x, is

$$\hat{x} = H^+ z.$$

In this proposed work, the residual vector R and the residual magnitude r shall be examined with respect to errors in measurements z and errors in the process model H. The concept is to not only identify where the errors arise, but also identify ways to correct the errors.

References [6, 17, 36-38] document state estimation as applied to power engineering, and errors in the state estimation process.

1.2 The theory of state estimation

State estimation is an increasingly common part of power utility energy management systems (EMSs). State estimation is a mathematical tool that is used to calculate voltage magnitude, phase angles, and other AC system variables from system measurements, such as complex power. State estimation is a software tool that relies on:

- Input data (measurements)
- Fundamental AC circuit laws
- The system model.

State estimation modules in EMSs are a *proven* technology that relies on redundancy of measurements, self-identification of problematic conditions, and bad data rejecting.

However, some state estimation accuracy affecting conditions have been known to exist, including: system blind spots, miscalibrated instruments, measurement error or bias, power system model errors, communication delay, communication channel bandwidth limits, and analog/digital (A/D) conversion resolution. If conditions exist that may affect state estimation accuracy, then it is important to characterize them for possible mitigation.

The most common state estimation method implemented by power utilities today is the weighted least squares (WLS) method, which is detailed in [17]. In essence, the WLS method is based on physical models for active and reactive power (P and Q). Measurements of P and Q are "forced" equal to calculated values from the physical model. The difference between the measurements and the model is called the residual. The residual is minimized in the least squares sense. The WLS has the ability to "flag" large measurement errors and, as an iterative process, may take more time to converge when error is present. However, some sources of error are small enough to escape notice and can lead to a persistent source of estimate accuracy degradation. Perhaps the greatest danger of error in state estimator input data relates to convergence. Figure 1.1 shows the generalized concept of nonlinear state estimation as applied in power engineering. The figure shows an iterative method for solving the nonlinear state estimation problem through recursive linearization. If the number of linearizations becomes large, it is assumed that the process is nonconvergent. If the input data has excessive error, the prospect of nonconvergence becomes a concern.

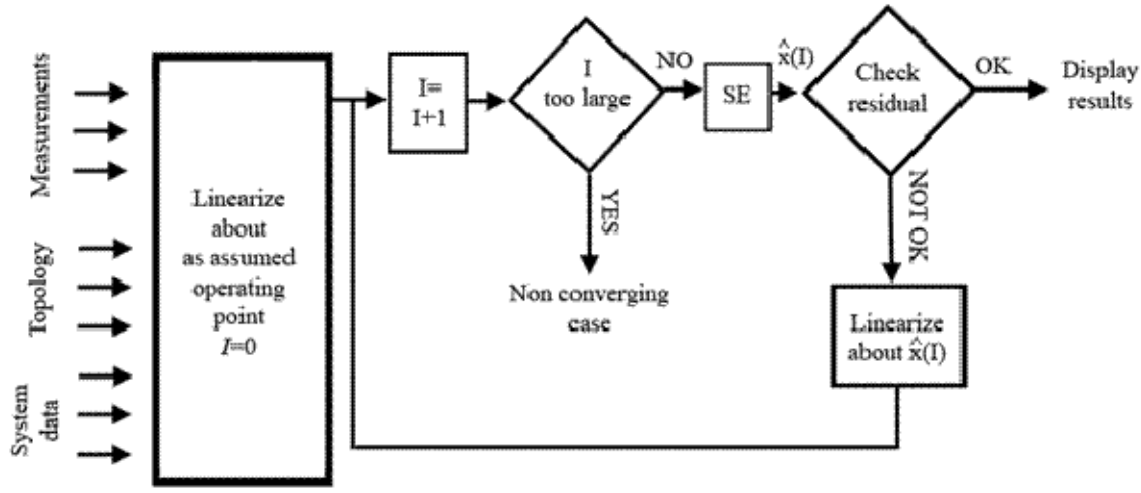

Figure 1.1 Pictorial of a recursive method for nonlinear state estimation

Another difficulty associated with state estimation is that SE, along with some other EMS calculations, traditionally utilizes a single-phase model to represent a multi-phase power system [29]. The single-phase power system model works well under symmetrical and balanced conditions. In the balanced instance, the negative and zero sequence currents and voltages are zero. This single-phase system can even produce acceptable answers when unbalance exists between the phases, providing zero and negative sequences are sufficiently small [12, 13]. However, unbalance between the three phases of a power system is the norm rather than the exception, for instance due to non-transposed transmission lines, single phase loads, or unbalanced loads [29]. These phenomena can lead to long convergence times, non-convergence, or inaccurate results in state estimation, if the unbalance is sufficiently severe.

State estimation can play a crucial part in the day-to-day operation of a power system utility. The system measurements are used for real-time operations like optimal power flow calculations. Proper system operation with regard to avoidance of insecure

conditions includes *situational awareness*; therefore the state estimator plays an important role in power system security. The importance of state estimators with regard to blackout avoidance is documented in [14]. A further motivation: in the increasingly deregulated power environment in the United States and abroad, more economic operation means savings for customers and power providers alike. Economic benefits might be realized if operators have a more accurate situational awareness of the system through improved state estimation.

1.3 Objectives

The main objective of this research is to identify some potential problems associated with common state estimation methods and to design "software fixes" or other solutions to these problems. The methods to improve state estimation and power system monitoring include:

- Accounting for measurements due to voltage and current instruments that are not collocated.
- Using unbalance factor values to improve model accuracy for power systems with three-phase measurements.
- Estimating measurement values in a system with non-simultaneous measurements.

1.4 Literature review

Power system state estimation is a documented subject that occupies a very large volume of technical literature. Classic papers on the subject include Schweppe's original paper on the subject and the paper that introduced Kalman filters [2], [3]. The method of

weighted least squares state estimation (WLS) is important because it is the method most implemented by power utilities today. Many state estimation textbooks go over the algorithm in detail, including reference [17]. The process will be outlined briefly later in this section.

There are many papers that concern measurement error and topology error identification in state estimation, particularly the weighted least square case. The error flagging and state identification properties of WLS SE make topology identification possible. One paper discusses comparing line measurements to well-observed adjacent measurements for spotting and correcting model parameter errors [4]. Another discusses using artificial neural networks to analyze unfiltered state estimation data for identifying and correcting topological and analytical errors [5]. Another paper that deals with finding topology errors is [6], where a residual sensitivity matrix W is compared to a measurement-to-branch matrix M. The idea behind this method is that single topology errors will have state estimation residuals that stand out from the rest of the system. The limitations of this system are discussed, as well as its application to real systems with possibly more than one topology error. The paper [7] is less general and discusses finding topology errors in power system state estimation by correlating measurements from suspected trouble-spots to those of known system anomalies, but only for single and multiple bus-split topology errors. The paper [8] presents an effective method for estimating a power networks topology in the presence of bad data and topology errors. This method tests measured real and reactive power flows with the WLS, but utilizing the Huber M-estimator method. In [9], the use of state-estimation for identifying topology errors is discussed in the instance of line or transformer outage, bus split and shunt capacitor/reactor switching.

The WLS method is a common type of state estimation and has been realized mathematically for single-phase and multi-phase power systems. The general WLS method contains a measurement vector *z*, a state vector *x*, a matrix *H* containing the coefficients that relate *z* and *x*, as well as the covariance matrix of measurement errors *R*. Figure 1.2 is a simple pictorial of the concept. The residual between the measured and estimated states is minimized iteratively by the following relationship,

$$\min J(x) = \min[z - [H]x]^T [R^{-1}][z - [H]x].$$

In typical single-phase power system usage, the measurements will be real and reactive power and the states will be bus voltages magnitudes and phase angles.

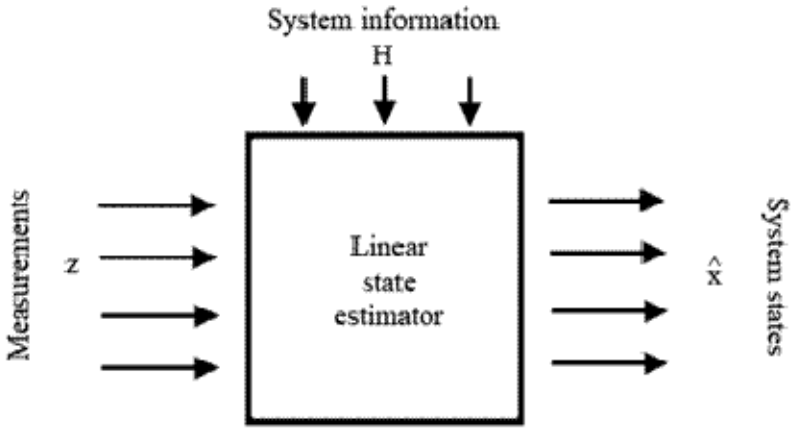

Figure 1.2 Pictorial of a state estimator

Examples of detailed three-phase least squares state estimation algorithms exist in the literature. There is a paper goes into detail on the modeling of many three-phase power system components and discusses a three-phase state estimation method similar to WLS [11]. Also discussed are the technologies available which make three-phase state estimation possible. A test bed is presented in reference [12] that shows the effect of measure-

ment noise on state estimation accuracy, with the conclusion that noise two times larger the meter accuracy has a profound effect against satisfactory measurement readings.

Unbalanced systems conditions occurring in three-phase state estimation have also been studied in the literature. A number of power systems are traditionally modeled in single-phase by utilizing the positive sequence components from three-phase measurements, even if a degree of unbalance is present. The paper [13] studies the error that occurs when a three-phase power system uses a single-phase model under unbalance conditions. The study uses an IEEE 30 bus system for a test model, where non-transposed lines or unbalanced loads are introduced with differing severity. Also present is random error in the systems power measurements. The result in each non-transposed lines case was bias in the final state estimation results and that modeling errors were not flagged by the state estimator. In the case of unbalanced loads with transposed lines, the error in the state estimation results were more severe. A 10% unbalance in one phase current resulted in skewed data similar to the worst non-transposed line case studied in this paper and the more unbalanced cased errors to increase significantly. While all of the non-transposed and unbalanced conditions resulted in a mismatch compared to "perfect" measurements, only the most extreme tested case of load unbalance was flagged as bad data by the state estimator.

This thesis presents the use of the unbalance factor to improve state estimation. Unbalance factor is calculated from the negative and positive components of voltage or current resulting from symmetrical transformation, where U_I is the current unbalance factor (CUF) and U_V is the voltage unbalance factor (VUF). The unbalance factor was first proposed as a ratio between the amplitudes of the negative and positive sequence voltage

or current [32], but has seen much more use lately as a complex ratio. The exact unbalance factor calculations are,

$$U_I = \frac{I_-}{I_+} \qquad \text{and} \qquad U_V = \frac{V_-}{V_+}.$$

There is very little in the literature about using unbalance factor values in state estimation. Unbalance factor is mainly used to quantify unbalance in a power system. Voltage unbalance factor is more often studied than current unbalance factor. The line-to-line voltage phasors always form a closed triangle and use of geometry and phasor mathematics can easily yield voltage complex unbalance factor, whereas current complex unbalance factor. Methods for calculating complex voltage unbalance factor from line-to-line voltage magnitudes are shown in [18], while line-to-neutral voltage magnitudes are shown to have calculable voltage angles in the absence of a zero-sequence component in reference [32]. Another paper details traditional methods used by utilities to measure unbalance factor and how this can be improved and used to represent line loss during unbalanced system conditions [19]. The reference [19] also mentions that the greatest cause of phase unbalance in a power system is single phase loads, such as AC railways or furnaces. Use of unbalance factor to describe the effects of these single-phase loads is documented in the literature, for instance a paper that discusses using unbalance factor to characterize the unbalance that can affect a single-phase load induction motor [20]. Despite all of these uses for complex unbalance factor, it is not a commonly metered quantity and requires special equipment or techniques.

Another potential problem facing state estimation is measurement timing. The state estimation algorithm depends on measurement inputs from throughout the system. If the states at time *t=0* are to be calculated, for example, then the measurements must

also be from time *t=0*, because old measurements may not accurately reflect the dynamic power system. Potential problems occur with this since power systems are often large entities, especially if you take into account separate, but interconnected, power systems. The communication system in this power system can sometimes report measurements from outlying instruments later than others [22]. The late measurement may be significantly late such that calculations like SE use a mix of new measurements and delayed measurements. Most SE algorithms assume no measurements are delayed, therefore error from the delayed measurements will be perceived as measurement error. Very complete state estimation models also take into account other interconnected power systems. Relying on the interconnected utility or a central power pool for measurements or state information may also add a time skew [23]. When collecting measurements for a state estimation calculation some of the measurements may be anywhere from 10 seconds to 60 minutes late (especially if waiting for state estimation results from a separate but interconnected power system) [23]. Suspected late measurements can be discarded from the SE, but this may result in poor performance [23]. It may be better to filter the suspected late measurements and some filtering methods will be discussed later in this section.

Measurement timing has seen much improvement in the past two decades. The Department of Defense's Global Positioning System (GPS) system is series of 24 satellites which can provide a time signal to an earthbound antenna that is accurate within 200 ns of Coordinated Universal Time (UTC) [10, 24]. Many power utilities are also having their proprietary measurement communication systems synchronized with GPS [25]. The GPS system is also an integral part of the PMU device and the GPS signal is the only re-

gional time source accurate enough to meet IEEE standards for real-time phasor measurements [24]. PMU devices measure voltage and current in three phases and return positive sequence phasor values, as well as time stamps for each measurement. This seems to offer a solution to time skew problems, since measurements could have their time stamps compared to see if any of them are "late", but that would require a significant amount of PMU coverage in a power system. However, most power systems have few PMUs, if any at all. Many studies have been done concerning the optimal placement of PMUs, such that total power system coverage is accomplished with a minimum of PMU units [26] and [27]. Were this implemented, time stamp solutions would be viable to the delayed measurement problem. PMU usage may see an increase in the future, since at least one protective relaying manufacturer (SEL, Pullman WA) now offers a PMU signal in most of its new relays. There is, nonetheless, a cost of communicating the PMU signal and integrating that signal into the software tools. Besides unit cost and time stamping, PMUs also seem to offer an advantage of additional measurements for the state estimation equation: phasor angles. However, the addition of phase angles to the measurement vector of WLS SE only increases SE confidence when the phase angle measurements are very accurate ($\delta_{Error} \leq 0.1^{\circ}$) [28].

PMUs use may not offer a practical solution to measurement time skew, but several computational algorithms exist to improve measurement data with time skew. Many studies have been done using Kalman filter algorithms to improve time skewed measurement data [23], [29]. The Kalman filter is a time-tested algorithm that can be used to account for noisy measurements when calculating states (and adopted to account for

measurement delay). Discrete Kalman filtering assumes the measurement signal can be estimated and the state calculated by the following equations,

$$\begin{aligned} x_{x+1} &= \phi_x x_k + w_k \\ z_k &= H_k x_k + v_k \end{aligned}.$$

In the previous equations, k is the time, x is the measurement vector, φ relates x_k to x_{k+1} (often the state transition matrix), and w is an assumed white noise component with known covariance structure. The state transition equations, with measurement vector z and coefficient matrix H, is familiar from WLS SE methods and this time includes a vector of measurement error v (white noise with known covariance structure and not coupled with w). The discrete Kalman filter loop is shown in Figure 1.3, where K is the Kalman gain, P is the error covariance matrix, Q is the expected value of noise w when squared, and R is the expected value of noise v when squared. A more detailed explanation of the Kalman filtering method can be found in [34]. The Kalman filter algorithm is often used to sort out measurement noise, and therefore has to be changed somewhat to handle delayed measurements. The literature presents a method for Kalman filtering against delays of a single sampling period that occur randomly with known probability [23] and times when the exact delay of each measurement is known [35].

Also present in the literature are algorithms less common than the Kalman filter used to account for delayed measurements. Presented in [22] are Winter's Multiplicative Seasonal Model and The Mixed Autoregressive-moving Average (ARMA). The Winter's Multiplicative Seasonal Model has three smoothing components, controlling the predicted mean, predicted slope, and a seasonal factor.

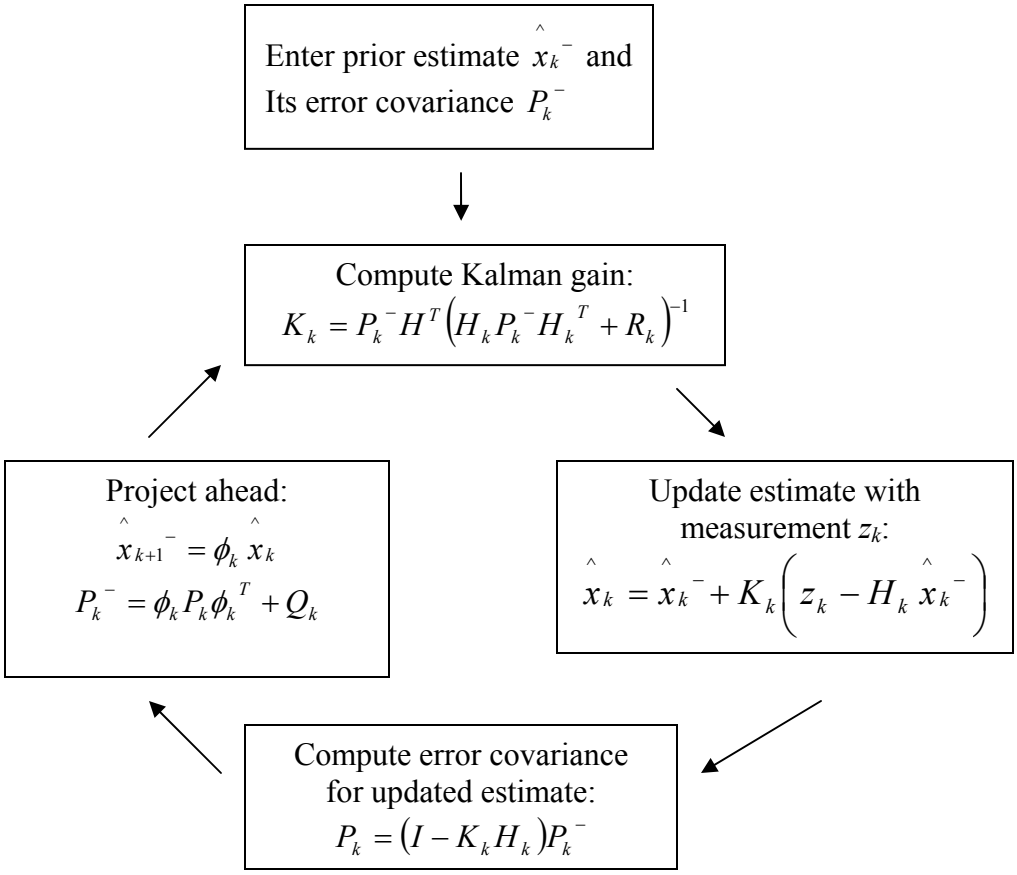

Figure 1.3 A flowchart illustrating the discrete Kalman filter loop

1.5 Organization of this thesis

This thesis is organized into five chapters:

1. State estimation introduction and literature review
2. Description and solution of the problem of non-collocated measurements for SEs.
3. Effects of voltage and current unbalance conditions on SE.
4. State estimation utilizing unsynchronized signals.
5. Conclusions and recommendations.

In addition, two appendices document the thesis. This is:

A: Guide to test case denomination and meaning.

B: Samples of MATLAB code used in this research.

CHAPTER 2 NON-COLLOCATED POWER MEASUREMENT CORRECTION

2.1 Non-collocated measurements

Complex power is a function of the complex voltage and current, where $S=VI^*$. Power measurement devices operate by sampling the voltage, *v(t)*, and the current, *i(t)*, which are converted to a digital signal by an A/D converter. The digital current and voltage signals are processed to obtain a product utilizing a power transducer. In the vast number of SE applications, the digital output of the power transducers is passed to a central computer via the Supervisory Control and Data Acquisition (SCADA) system. The power transducers send signals every Δt seconds where Δt is typically in the 1 to 5 second range. The SCADA system has been designed to accommodate the power transducer signals in addition to the many other signals passed through this data acquisition hardware. Also, voltage magnitude and current magnitude signals may be obtained from A/D transducers, and, again, passed to the central computer via the SCADA system. In recent years, a new device has been augmented into the traditional system described: this is the phasor measurement unit. A PMU is capable of calculating the phase of voltage and current measurements, and these signals are available at relatively high sample rates (e.g., 1 second). At the time of writing, few electric utility companies have installed PMUs. However, there is a clear trend and thrust to radically increase the number of PMUs in power systems. Because PMUs are GPS based devices, they are capable of time stamping measurements. Because phase angles of V and I are available in PMUs, complex power $P+jQ$ may be readily calculated. An example of a power measurement instrument setup is shown in Figure 2.1. In this figure, a PMU is shown. In the large majority of

power systems, PMUs are not used: in these cases, P and Q measurements are simply passed to the SCADA system. When measuring or calculating complex power, the voltage and current must be taken from the same place in the system. In the case of a non-collocated power measurement, this is not the case. The impedance between the CT and PT can be represented as the circuit shown in Figure 2.2. In the case of a non-collocated measurement it is assumed that the instruments are not far apart and well within the range of typical short line modeling limits. Because the CT and PT are often not separated by even a kilometer, resistance in the impedance model has been assumed to be negligible. An example of a non-collocated instrument placement is shown in Figure 2.3.

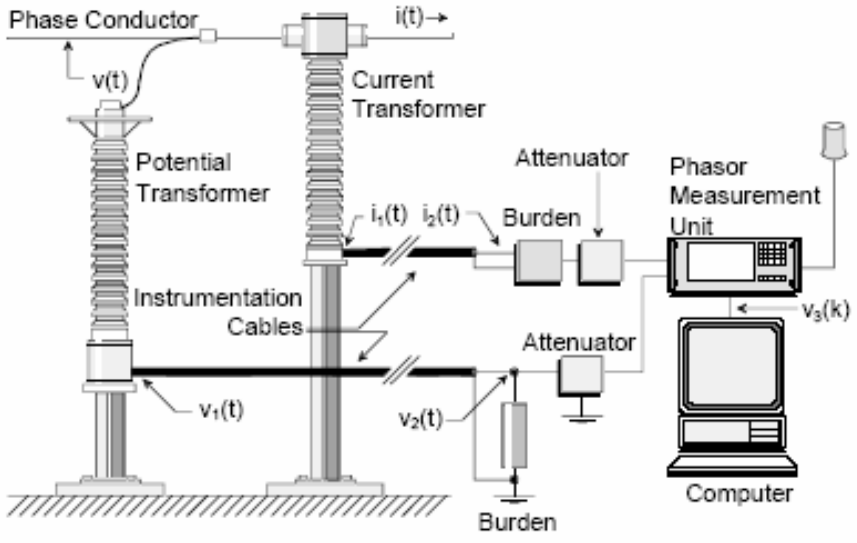

Figure 2.1 An example of a complex power measurement setup
taken from [1]

When discussing power values in this paper, the notation S_{ab} will be used. The subscript a will be the same subscript as the voltage used to calculate S_{ab} and the subscript b will be the subscript of the current used to calculate S_{ab}. For instance, meaningful power values from the system in Figure 2.2 would be S_{11} and S_{22}, which are calculated as follows,

$$S_{11} = V_1 I_1^*$$

$$S_{22} = V_2 I_2^*.$$

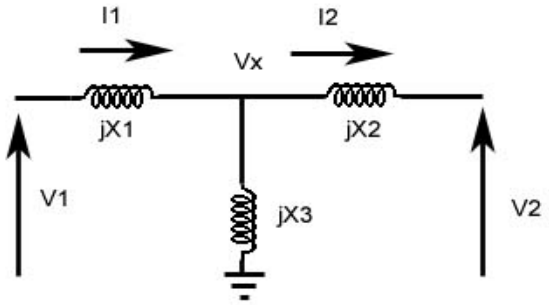

Figure 2.2 A model for the reactance between CT and PT in a non-collocated measurement

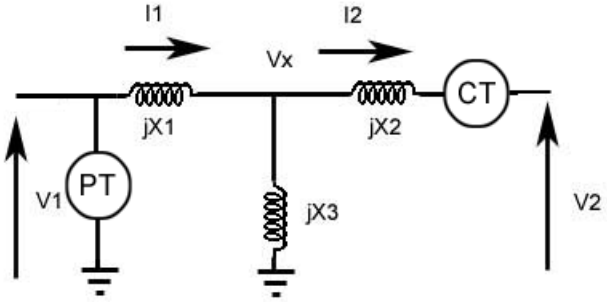

Figure 2.3 An example of a non-collocated power measurement instrument placing

Note that in the S_{11} and S_{22} expressions, the notation V, I, and S are complex numbers (i.e., sinusoidal steady state, phasor, analysis). The notation $|\cdot|$ shall be used to denote amplitude. Examples of non-collocated power measurements from the system in Figure 2.2 would be S_{12} (shown with instrument placing in Figure 2.3) or S_{21}. Each of these is calculated as follows,

$$S_{12} = V_1 I_2^*$$

$$S_{21} = V_2 I_1^*.$$

Complex power calculations can be put into a general matrix form, where V is a vector of complex voltage values at a bus (sinusoidal steady state, phasor notation) and similarly, let I be a vector of line currents. The dimensions of these vectors are N_V and N_I, respectively. Further, there is a complex power matrix of dimension N_V by N_I defined as

$$S = VI^H .$$

where $(\cdot)^H$ denotes the hermitian operation (complex conjugate followed by a transpose). Then elements of matrix S in positions like S_{aa} represent the familiar conventional complex power. However, elements like S_{ab}, $a \neq b$, represent non-collocated signals that are dimensionally like $P + jQ$, but do not represent conventional active and reactive power. The issue is the 'correction' of non-collocated terms like S_{ab} to obtain conventional active and reactive power like S_{aa}. Consider the case that $N_V = N_I = 2$, and the current vector I is written with polarity such that both currents are input to the two-port network. Then it is a simple matter to show that

$$S = VI^H = ZII^H = VV^HY^H$$

where Z and Y are the bus impedance and admittance matrices of the two-port. The use of Z and Y imply that the bus current injection vector is $[I_1 \; -I_2]^t$ in the notation of Figure 2.2. Note that S is a complex, non-symmetric matrix which can easily be shown to be of deficient rank and hence $S_{11}S_{22} = S_{12}S_{21}$. There is a similar quantity s defined as $s = I^HV$ which is a scalar complex quantity that has the property $\mathrm{Re}\{s\} \geq 0$ for a passive two-port. This property can be used to demonstrate that the bus impedance and admittance matrices are positive real matrices [39]. The following correction method has been submitted for

IEEE publication as a letter [40] and this chapter was presented at the 2005 North American Power Symposium[41].

It is possible to calculate all of the power, voltage, and current values of the circuit in Figure 2.2 (including S_{11} and S_{22}) given only the systems reactance, X_1, X_2, and X_3, a voltage magnitude, $|V_1|$ or $|V_2|$, and a non-collocated complex power measurement, S_{12} or S_{21}, which are values relative to the circuit shown in Figure 2.2. This can be done using one of two methods: Case A and Case B, which will be detailed in this section. Case A is for instances when the voltage magnitude component of the non-collocated power is known and Case B is used when a voltage magnitude is know that is not part of the non-collocated power value.

One method for correcting non-collocated measurements will be called the "Case A" method. For Case A, a voltage magnitude is known and is a component of the non-collocated power measurement. First a method will be shown where S_{12} is known, as well as $|V_1|$, X_1, X_2, and X_3. S_{11} and S_{22} will be shown to be calculable from these values. This method can also be changed to work with S_{21} and $|V_2|$ being known values, which will be explained later. The voltage magnitude V_1 can be made the reference voltage, therefore,

$$V_1 = 1\angle 0^\circ .$$

Since $S_{12} = V_1 I_2^*$ and S_{12} and V_1 is known, I_2 can be calculated immediately.

$$I_2 = \frac{S_{12}^*}{V_1^*}$$

To calculate S_{11} and S_{22}, V_2 and I_1 are needed. The following matrix equation can be formed to solve for the remaining unknowns,

$$\begin{bmatrix} V_1 \\ V_2 \end{bmatrix} = j \begin{bmatrix} X_1 + X_2 & X_2 \\ X_2 & X_2 + X_3 \end{bmatrix} \begin{bmatrix} I_1 \\ -I_2 \end{bmatrix}. \qquad (2.1)$$

Equation 2.1 are a simple consequence of the bus impedance analysis of a linear AC circuit, namely $V_{bus} = Z_{bus} I_{bus}$, where Z_{bus} is the bus impedance matrix referred to ground [8]. The impedance has been simplified into reactance for use with the non-resistive model.

Equation 2.1 can be multiplied out to give two equations that can be solved for the two unknowns, V_2 and I_1. Solving for V_2 and I_1 yields the following equations,

$$\frac{1}{j(X_1 + X_3)} \begin{bmatrix} jX_3 & X_1X_2 + X_1X_3 + X_2X_3 \\ 1 & jX_3 \end{bmatrix} \begin{bmatrix} V_1 \\ I_2 \end{bmatrix} = \begin{bmatrix} V_2 \\ I_1 \end{bmatrix}.$$

The matrix relationship simplifies into the following

$$V_2 = \frac{jX_3V_1 + I_2(X_1X_2 + X_1X_3 + X_2X_3)}{j(X_1 + X_3)}$$

$$I_1 = \frac{V_1 + jX_3I_2}{j(X_1 + X_3)}$$

This Case A method can be changed to apply to when S_{21} and $|V_2|$ are known. The diagram in Figure 2.4 shows how the polarities of these values are changed using Case A with these numbers. The preceding method can be used, but V_2 is used in place of V_1, V_1 is used in place as V_2, I_2 is replaced by $-I_1$, I_1 is replaced by $-I_2$, X_2 is used for X_1 and X_1 is used for X_2. For instance, in the first step of Case A, it is $|V_2|$ that becomes the reference voltage instead of $|V_1|$. V_2 and S_{21} next solve for $-I_1$, as another example. A detailed guide for parameter replacement is shown in Table 2.1.

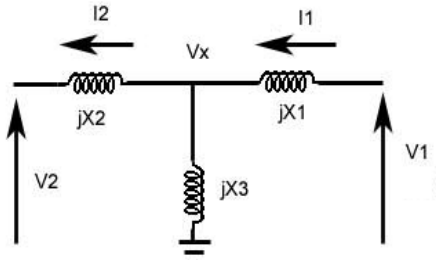

Figure 2.4 A circuit diagram showing how the V_2, S_{21} case is similar to Case A

Table 2.1 A parameter replacement guide to use Case A with S_{21} and V_2 known or Case B with S_{12} and V_2

Parameter	Replace With
V_1	V_2
V_2	V_1
I_1	$-I_2$
I_2	$-I_1$
X_1	X_2
X_2	X_1
S_{21}	S_{12}
S_{12}	S_{21}

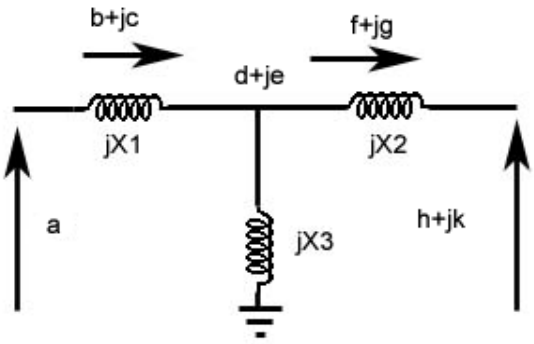

Figure 2.5 A new notation for the non-collocated impedance model for use in Case B

The next method is called the "Case B" method. This method is uses when a voltage magnitude is known, but that voltage is not part of the non-collocated power calculation. The method shown is for when S_{21} and $|V_1|$ are known, along with the reactance

X_1, X_2, and X_3. It will later be shown how Case B can solve for the instance where S_{12} and $|V_2|$ are known later in this section.

Since one of the current cannot be immediately calculated with the given voltage and non-collocated power, Case B is discussed separately. To solve for S_{11} and S_{22}, a new circuit model is needed, shown in Figure 2.5.

The given voltage is again the reference voltage, therefore using the new notation given in Figure 2.5,

$$V_1 = |V_1| \angle 0° = a \, .$$

Using basic power relationships, where $S=VI^*$, $P=Real\{S\}$, and $Q=Imag\{S\}$, the following relationships can be made using the new notation

$$P_{11} = ab$$

$$Q_{11} = -ac$$

$$P_{22} = hf + kg$$

$$Q_{22} = kf - hg$$

$$P_{21} = hb + kc$$

$$Q_{21} = bk - hc \, .$$

The parameters a, P_{21}, and Q_{21} are known values. To help solve for the remaining unknowns, additional equations can be written using the relationships between V_1 and V_X, V_X and V_2. These are written using the Kirchhoff laws,

$$\begin{aligned} d + je &= a - (b + jc)(jX_1) \\ h + jk &= d + je - (f + jg)(jX_2) \end{aligned}$$

$$b + jc = \frac{d + je}{jX_3} + f + jg \, .$$

Here X_1, X_2, X_3, and a are known values. Using these equations and the power relationships, there are eight equations with eight unknown parameters. The eight equations can be simplified even more to the following

$$d = a + cX_1$$

$$e = -bX_1$$

$$h = d + gX_2$$

$$k = e - fX_2$$

$$b = f + \frac{e}{X_3}$$

$$c = g - \frac{d}{X_3}$$

$$P_{21} = hb + kc$$

$$Q_{21} = bk + hc\,.$$

Solving for the unknown parameters is a simple but time consuming process and left as an exercise for the reader. Once all of the parameters in Figure 2.5 are solved for, the real and unreal parts of S_{11} and S_{22} can be calculated with the following equations,

$$P_{11} = P_{21}\left(\frac{X_3}{X_3 + X_2}\right)$$

$$a = V_1 = 1\angle 0°$$

$$b = P_{11} = P_{21}\left(\frac{X_3}{X_3 + X_2}\right)$$

$$k = \frac{-P_{21}}{(X_2 + X_3)}(X_3X_1 + X_2X_3 + X_1X_2)$$

$$Q_{11} = -\left(\frac{P_{21} - \sqrt{{P_{21}}^2 - 4k^2b^2 + 4kbQ_{21}}}{2k}\right)$$

$$S_{11} = P_{11} + Q_{11}$$
$$I_1 = \frac{S_{11}^*}{V_1^*}$$
$$V_2 = \frac{S_{21}}{I_1^*}$$

$$I_2 = I_1 - \frac{V_1 - jX_1 I_1}{jX_3}.$$

The Case B method equations shown directly above can also be used when S_{12} and V_2 are known. The diagram in Figure 2.4 shows how the polarities of these values are changed using Case B with these numbers. The Case B method can be used, but V_2 is used in place of V_1, V_1 is used in place as V_2, I_2 is replaced by $-I_1$, I_1 is replaced by $-I_2$, X_2 is used for X_1 and X_1 is used for X_2. For instance, in the first step of Case A, it is $|V_2|$ that becomes the reference voltage instead of $|V_1|$. V_2 and S_{21} next solve for $-I_1$, as another example. A detailed guide for parameter replacement is shown in Table 2.1, which works for Case A and Case B.

Case A and Case B show that complex power can be calculated from a non-collocated measurement. A local voltage measurement and a detailed model of the local impedance are required along with the non-collocated power measurement.

2.2 Illustrative examples

To illustrate the effect of non-collocated power measurements, an 11 bus test bed has been created. The test bed has been loosely based on the 500 kV transmission line grid in the United States southwest. The reactance and network configurations have been "invented" to obtain a convenient test bed and are shown in detail in Figure 2.6. The black diamonds in Figure 2.6 represent wattmeters. Line parameters were calculated

from the actual line configurations and approximate line length. These parameters are shown in Table 2.2 in per unit on a 100 MVA, 500 kV base. Each bus was assigned a per unit voltage value. Knowing the bus voltage and line parameters allowed calculation of the individual line currents and complex power flow.

The state estimation calculations using the 11 bus system data was performed using Matlab mathematical software, with sample code of these calculations provided in Appendix B. The goal of the examples discussed below is to examine the error in state estimation that may occur from a non-collocated power measurement and to show the benefit that may be gained from correcting them. Different test cases will be examined and these cases will be outlined later in this chapter, in Table 2.4, and in Appendix A.

Table 2.2 Line reactance for the Case 0-4, 11-bus test bed, on a 100 MVA, 500 kV base

Line Parameter	Reactance (p.u.)
Xa	0.017
Xb	0.004
Xc	0.0335
Xd	0.0015
Xe	0.0062
Xf	0.0483
Xg	0.0064
Xh	0.0206
Xj	0.0039
Xk	0.0099
Xl	0.0156

The test bed uses 18 power instruments whose readings are used in state estimation to calculate the voltage angle and voltage magnitude at each bus. The location of these power instruments are depicted in Figure 2.6 using black diamonds. WLS state estimation is the most common form of state estimation used by power utilities and will be used in this example. Least squares state estimation multiplies a vector of measurements

[z] to the pseudo-inverse of the process matrix [H], which gives a state estimate vector [x]. The matrix [H] is a matrix of coefficients that is N_m (the number of measurements) by N_s (the number of states). Least squares state estimation is improved by a large number of measurements and in power engineering the case is always overdetermined, where $N_m > N_s$. The final unweighted, overdetermined case is shown here

$$[x] = \left[[H]^T [H] \right]^{-1} [H]^T [z].$$

For calculating the bus angles with real power measurements, the following power flow equation is used,

$$P = \frac{|V_1||V_2|}{X} \sin(\delta_1 - \delta_2).$$

Since the voltages are all very close to 1.0 per unit during the steady state and the angles very close to zero, the general power flow equation can be simplified. The sine of small angles is approximately the angle itself. The following power equation is used,

$$P = \frac{1}{X}(\delta_1 - \delta_2).$$

In the context of least squares state estimation, the matrix [z] is made of real power measurements and the matrix [H] is made from the inverses of the line reactance. The state matrix [x] is composed of the bus reference angles to be estimated.

Now the state estimation equation for the reactive power is created. Again voltages are assumed to be very close to 1.0 per unit value and the reference angles close to zero. The equations can be simplified as follows,

$$V_1 = 1 + \Delta V_1$$

$$V_2 = 1 + \Delta V_2$$

$$Q = \frac{|V_1|^2 - |V_1||V_2|\cos(\Delta\delta)}{X} \approx \frac{1}{X}\left[\Delta V_1 - \Delta V_2\right].$$

Whether calculating voltage magnitude or angle, the [*H*] matrix can be made from the inverse of each lines reactance. Here the measurement vector [*z*] is the reactive power measurements and the state vector [*x*] is made of bus voltage magnitudes.

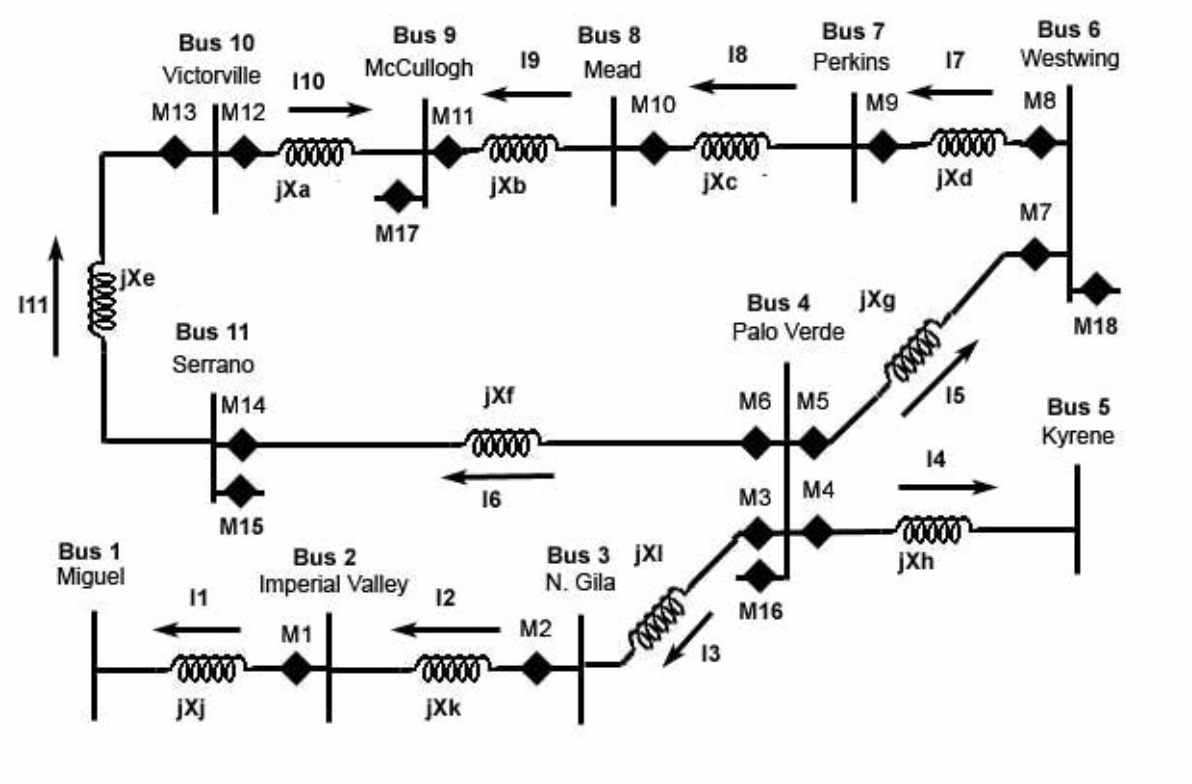

Figure 2.6 An 11 bus test bed inspired by the 500 kV lines of the US southwest

It should be mentioned that the WLS state estimation method is an iterative process. The state vector *x* is guessed at and then compared to the $\hat{x}$ value calculated from the *H* matrix and *z* measurement vector. The difference between *x* and $\hat{x}$ occurs from measurement error, symbolized as η, where,

$$\hat{x} = H^{+}\left(z + \eta\right).$$

The iterative process updates H and z until the difference between $\hat{x}$ and $\hat{x}$ from the previous iteration is small. In these WLS state estimation calculations performed on the 11 bus test system and in the WLS calculations performed throughout this entire thesis, only the first iteration results are considered. The H matrix, computed as states above, will be used on the measurement vector z directly to calculate $\hat{x}$. The measurement-correction techniques derived here and throughout this thesis are designed to produce better first iteration results. Only the first iteration results are considered for this thesis and this is because:

- An iterating state estimator adds a significant level of variables to the given problems.
- It is assumed a first iteration state estimation result closer to the true state value will produce better results and/or and answer in fewer iterations in an iterating state estimator.

As for the non-collocated measurement element to this test, the test bed will have an introduced non-collocated measurement at Bus 2 for the non-collocation case studies. The impedance used in all instances is shown in Table 2.3, relative to the general non-collocated impedance circuit shown in Figure 2.2. The X_1 and X_2 impedance values could represent large series capacitors, where X_3 is a shunt reactance. The non-collocated power instrument will calculate power from the V_2 and I_1 positions, relative to the diagram in Figure 2.2. The power at instrument *M1* should read 5.14 per unit, but in this non-collocated instance it reads 1.05 per unit.

Table 2.3 Test bed reactive values for testing non-collocated measurements in Cases 1-4, relative to circuit in Figure 2.1, on a 100 MVA and 500 kV base

	Value in per unit
X_1	-0.01022
X_2	-0.00995
X_3	0.87719

The test will be conducted in five cases, denominated Cases 0, 1, 2, 3, and 4. The details of these cases as well as all the test cases in this report appears in Appendix A. For each case, the complex power measurements are used to calculate the state variables δ and $|V|$. The objectives and generalized descriptions of the six cases appear in Table 2.4. The state variables will have the no-error, no non-collocation Case 0 results subtracted from them, giving δ-$\delta_{no\text{-}error}$ and $|V|$-$|V|_{no\text{-}error}$ for each case. The δ-$\delta_{no\text{-}error}$ and $|V|$-$|V|_{no\text{-}error}$ values will be calculated 1000 times and the average value will be analyzed by observing the 2-norm residual, mean, and variance. The Case 0 has no power measurements error and no non-collocated instruments, and therefore the δ-$\delta_{no\text{-}error}$ and $|V|$-$|V|_{no\text{-}error}$ values are expected to be close to zero. Case 1 has power measurements with Gaussian distributed error of 10% and no non-collocated power instruments. Case 2 has power measurements with Gaussian distributed error of 30% and have no non-collocated power measurements. Case 3 has power measurements with a Gaussian distributed error of 10%, and one non-collocated power instrument at Bus 2. Case 4 has power measurements with Gaussian distributed error of 30% and one non-collocated power instrument at Bus 2. The percent error used are representative of random error in power systems measurements. It is hoped that by comparing Cases 0, 1, 2, 3 and 4 that the amount of error due to random noise (the percent error in cases 1, 2, 3, and 4) and the non-

collocated instrument (Cases 3 and 4 only) can be discerned. The results of test cases 0-4 are shown in Tables 2.5, 2.6, 2.7, and 2.8.

Table 2.4 State estimation Cases 0-4 testing criteria used with the 11 bus test bed

Case	Objective	Measurement noise	Non-collocated measurement
0	Base case	None	No
1	Low noise case	10%	No
2	High noise case	30%	No
3	Low noise, non-collocated measurement	10%	One, located at bus 2
4	High noise, non-collocated measurement	30%	One, located at bus 2

Table 2.5 Test bed average δ after 1000 runs compared to actual δ, for Cases 0-4

		State δ-$\delta_{\text{no-error}}$		
Case	Noise	$\|\|r\|\|_2$ of δ (rad)	Mean (rad)	Variance (rad)
0	none	0.0945948	0.028521	1.62E-32
1	10%	0.0945958	0.028521	5.13E-09
2	30%	0.094598	0.028521	5.26E-08
3	10%, one non-collocated measurement	0.095822	0.028521	2.39E-05
4	30%, one non-collocated measurement	0.09586	0.028521	2.43E-05

Table 2.6 Test bed average $|V|$ after 1000 runs compared to actual $|V|$, for Cases 0-4

		State $\|V\|$-$\|V\|_{\text{no-error}}$		
Case	Noise	$\|\|r\|\|_2$ of $\|V\|$ (p.u. volts)	Mean (p.u. volts)	Variance (p.u. volts)
0	none	0.081075	-0.022879	8.18E-05
1	10%	0.081079	-0.022879	8.20E-05
2	30%	0.081119	-0.022879	8.11E-05
3	10%, one non-collocated measurement	0.081558	-0.022879	8.88E-05
4	30%, one non-collocated measurement	0.081511	-0.022879	8.92E-05

Table 2.7 Test bed average P measurement after 1000 runs compared to actual P, for Cases 0-4

		P-$P_{\text{no-error}}$		
Case	Noise	$\|\|r\|\|_2$ of P (p.u.watts)	Mean (p.u. watts)	Variance (p.u. watts)
0	none	0.098162	-0.003115	5.57E-04
1	10%	0.107574	-0.006990	9.39E-04
2	30%	0.239030	-0.035610	0.002054
3	10%, one non-collocated measurement	4.101085	-0.2225	0.929933
4	30%, one non-collocated measurement	4.101085	-0.2225	0.934167

Table 2.8 Test bed average Q measurement after 1000 runs compared to actual Q, for Cases 0-4

		Q-$Q_{\text{no-error}}$		
Case	Noise	$\|\|r\|\|_2$ of Q (p.u. vars)	Mean (p.u. vars)	Variance (p.u. vars)
0	none	1.676460	0.008759	0.165243
1	10%	1.447761	0.086734	0.115952
2	30%	1.448581	0.084969	0.1149
3	10%, one non-collocated measurement	2.16158	-0.006283	0.274566
4	30%, one non-collocated measurement	2.155998	-0.003878	0.275201

2.3 Observations drawn from the example

The complex power in each test case is shown in Tables 2.7 and 2.8. In general, the random measurement error in Cases 1 and 2 increases the 2–norm residual for P-$P_{\text{no-error}}$ and the mean of P-$P_{\text{no-error}}$ for the active power deviates from zero (relative to the no-error Case 0). For both the real and reactive power comparisons, the variance increases due to measurement error. Subsequently, the measurement error alone increases overall measurement error and variance. Cases 3 and 4 possess measurement error and a single

non-collocated measurement. In Cases 3 and 4 the P-$P_{\text{no-error}}$ and Q-$Q_{\text{no-error}}$ values result in a 2-norm residual at least two orders of magnitude larger than the error associated with the no-error Case 0. The mean value of P-$P_{\text{no-error}}$ also increases for the non-collocated test cases 3 and 4 (relative to Case 0). There also exists larger variance relative in cases 3 and 4 relative to Cases 0, 1 and 2, for real and reactive power differences and state differences. Because of the increased P-$P_{\text{no-error}}$ and Q-$Q_{\text{no-error}}$ error in Cases 3 and 4, as well as an overall variance increase in the Cases 3 and 4, it can be said that a single non-collocated instrument increased the measurement error in the test bed and the variance.

The effect of the non-collocated measurements on the estimation of states is more subtle than the effects on the direct power measurements. The means differences in state values from the no-error case are shown in Tables 2.5 and 2.6. Tables 2.5 and 2.6 show that Cases 1 and 2, which contain only measurement error, differ little from the no-error Case 0. The only exception to the forgoing is a marked increase in variance in the δ-$\delta_{\text{no-error}}$ calculations in Cases 1 and 2 relative to Case 0. Measurement error alone then only introduces variability into the bus phase angle calculations. When a single non-collocated measurement is added during Cases 3 and 4 the result is a small 2-norm residual increase and variance increase for the δ-$\delta_{\text{no-error}}$ and $|V|$-$|V|_{\text{no-error}}$ measurements relative to Cases 0, 1 and 2. The variance change is smaller for the $|V|$-$|V|_{\text{no-error}}$ measurement than it is for the δ-$\delta_{\text{no-error}}$ measurement. The preceding observations show that in power system state estimation, a single non-collocated instrument can increase the variance of calculated bus voltage angles and magnitudes and thus increase error in the estimate.

Applying the non-collocated measurement calculations discussed in Section 2.1 eliminates the non-collocated error. In this case, since the non-collocated power is calcu-

lated from V_2 and I_1, then Case B from Section 2.1 would be the appropriate "fix." The "fix" (i.e., mathematical correction) is a software fix. After the power measurement adjustment, the Case 3 and 4 results would resemble the Cases 1 and 2 results. By comparing Cases 1 and 2 to Cases 3 and 4, the benefits become apparent: there is a lower amount of estimate variance and a lower 2-norm residual in Cases 1 and 2. Therefore, accounting for non-collocated measurement increases state estimation confidence and creates more accurate measurements system-wide.

CHAPTER 3 UNBALANCE FACTOR USE FOR SINGLE PHASE STATE ESTIMATION IMPROVEMENT

3.1 Complex voltage and current unbalance factor

The voltage and current unbalance factors are a way of quantifying unbalance in a three-phase power system. The three-phase current or voltage values can be decoupled into the positive, negative, and zero-sequence components through the symmetrical component transformation.

$$\begin{bmatrix} V_a \\ V_b \\ V_c \end{bmatrix} = [M] \begin{bmatrix} V_+ \\ V_- \\ V_0 \end{bmatrix} \quad , \quad \begin{bmatrix} I_a \\ I_b \\ I_c \end{bmatrix} = [M] \begin{bmatrix} I_+ \\ I_- \\ I_0 \end{bmatrix},$$

$$a = 1\angle 120° = -\frac{1}{2} + j\frac{\sqrt{3}}{2} \ ,$$

$$M = \frac{1}{\sqrt{3}} \begin{bmatrix} 1 & 1 & 1 \\ a^2 & a & 1 \\ a & a^2 & 1 \end{bmatrix} \qquad \text{and} \qquad M^{-1} = \frac{1}{\sqrt{3}} \begin{bmatrix} 1 & a & a^2 \\ 1 & a^2 & a \\ 1 & 1 & 1 \end{bmatrix}.$$

The unbalance factor is a complex quantity used to quantify the amount of unbalance in a power system, and is computed from the positive and negative sequence values,

$$U_I = \frac{I_-}{I_+} \qquad \text{and} \qquad U_V = \frac{V_-}{V_+}.$$

Under balanced conditions, $U_I = U_V = 0$. Typically traditional power system instrumentation does not measure unbalance factor directly and software techniques are required. However, many proposed methods exist for calculating the complex unbalance factor in a system [16, 18], but this is often only for the voltage unbalance factor. It is also possible

to directly calculate the current or voltage complex unbalance factor if complete three-phase phasor measurements are available, however this is rarely the case.

In many routine power engineering calculations, balanced conditions are assumed [12, 13]. In a balanced three-phase power system, the negative and zero sequence values are zero. This effectively simplifies a three-phase system into a single-phase system for the purposes of various calculations. However, unbalanced conditions with negative and zero sequence components are a reality in modern power systems [29]. There are many causes of system unbalance, for instance single-phase loads and untransposed power lines on crowded rights-of-way. Single-phase methods for state estimation can still prove effective even when unbalanced conditions are present in a small degree, but some power systems may have enough unbalance to warrant a state estimation solution that takes into account system unbalance. In communication with a major U. S. utility company, it is found that only positive sequence voltages and currents are commonly reported and the SCADA system, and therefore $P+jQ$ is derived usually from $(V_+)(I_+^*)$. That is, negative and zero sequence signals are ignored. Examples of the effect of unbalanced operation in traditional state estimation calculations exist where the unbalance is taken from real data and the effect on state estimation is noticeable [13]. This thesis seeks to use the unbalance factor measurements in a power system to improve state estimation calculations, utilizing their positive and negative sequence information.

Complex power measurements are often used in EMS state estimation programs to find other values in a power system, like bus voltage magnitudes and bus angles. As it has been stated earlier in this section, it is not uncommon for power utilities to operate under a positive-sequence-only assumption for routine calculations. Some power utilities

may also only be monitoring a single phase at any point in the power system. If there are only positive-sequence values in the system, then monitoring the voltage, current, and complex power flow in a single phase is enough to calculate current, voltage, and complex power in the two other phases through symmetrical component transformation. When calculating the total, three-phase power flow at a point, the complete definition is as follows,

$$S_{3\phi} = S_{Total} = V_{an} I_a^{\ *} + V_{bn} I_a^{\ *} + V_{cn} I_a^{\ *}$$
$$S_{Total} = V_{+} I_{+}^{\ *} + V_{-} I_{-}^{\ *} + V_0 I_0^{\ *}.$$

This is true when the symmetrical component transformation matrix, M, is a hermitian matrix, where $M^{-1}=M^H$, as follows,

$$M = \frac{1}{\sqrt{3}} \begin{bmatrix} 1 & 1 & 1 \\ a^2 & a & 1 \\ a & a^2 & 1 \end{bmatrix}.$$

When there is a positive-sequence-only assumption, the negative and zero sequence components are zero and the total complex power can be expressed more simply as,

$$S_{3\phi} = S_{Total} = V_{+} I_{+}^{\ *} = V_{an} I_a^{\ *} + V_{bn} I_a^{\ *} + V_{cn} I_a^{\ *}. \qquad (3.1)$$

This three-phase power value in Equation (3.1) is correct in the balanced case. In the proposed case of significant system unbalance, the value calculated in Equation (3.1) is missing negative and zero sequence information.

If the power system has a significant negative sequence voltage and current, but still a negligible zero-sequence component, then using the unbalance factor can lead to an accurate, or at least improved (if a small amount of zero sequence current or voltage are

available), complex power value, $S_{3\phi}$. It is said that zero-sequence components are small regardless of the amount of unbalance present [16]. This is often the case since many power transmission and distribution systems employ delta connected transformers which block zero sequence components. A more accurate $S_{3\phi}$ value, which has negative sequence information, will then result in a more accurate set of results in state estimation. This three-phase power calculation which features negative sequence information will be as follows,

$$S_{3\phi} = S_{Total} = V_+ I_+^* + V_- I_-^* = V_{an} I_a^* + V_{bn} I_a^* + V_{cn} I_a^*.$$

Negative and positive sequence values can now be related to the unbalance factor, as follows,

$$\begin{bmatrix} V_{an} \\ V_{bn} \\ V_{cn} \end{bmatrix} = \frac{1}{\sqrt{3}} \begin{bmatrix} 1 & 1 & 1 \\ a^2 & a & 1 \\ a & a^2 & 1 \end{bmatrix} \begin{bmatrix} V_+ \\ V_- \\ 0 \end{bmatrix}$$

$$V_{an} = \frac{1}{\sqrt{3}}(V_+ + V_+ U_V) = \frac{1}{\sqrt{3}} V_+ (1 + U_V) \tag{3.2}$$

$$V_{bn} = \frac{1}{\sqrt{3}}(a^2 V_+ + a V_+ U_V) = \frac{1}{\sqrt{3}} V_+ (a^2 + a U_V) \tag{3.3}$$

$$V_{cn} = \frac{1}{\sqrt{3}}(a V_+ + a^2 V_+ U_V) = \frac{1}{\sqrt{3}} V_+ (a + a^2 U_V) \tag{3.4}$$

It will be assumed that only single-phase information is available from system measurements (phase *a*). It will also be assumed that unbalance factor values are available. Given these assumptions, there are three equations, Equations (3.2), (3.3), (3.4), with

three unknowns, V_+, V_{bn}, and V_{cn}. Solving Equations (3.2), (3.3) and (3.4) for the unknowns yields,

$$V_+ = \frac{\sqrt{3}V_{an}}{1+U_V}$$

$$V_{bn} = \frac{V_{an}}{1+U_V}(a + a^2 U_V)$$

$$V_{cn} = \frac{V_{an}}{1+U_V}(a^2 + aU_V)\,.$$

Now all the voltages in the system are expressible with unbalance factor values and V_a. If all of the current values could be expressible with unbalance factor and the known single-phase measurement I_a, then $S_{3\varphi}$ can be calculated exactly given the no zero-sequence assumption. The symmetrical component transformation for current is the same as it is for voltage and the unknown current values I_b, I_c and I_+ can be derived the same way as the unknown voltage-based values. This results in the following equations,

$$I_+ = \frac{\sqrt{3}I_a}{1+U_I}$$

$$I_b = \frac{I_a}{1+U_I}(a + a^2 U_I)$$

$$I_c = \frac{I_a}{1+U_I}(a^2 + aU_I)\,.$$

Using the above derived relationships, the complex power $S_{3\phi}$ is reevaluated in known terms,

$$S_{3\phi} = V_{an}I_a^{\,*} + \frac{V_{an}}{1+U_V}(a + a^2 U_V)\frac{I_a^{\,*}}{1+U_I^{\,*}}(a + a^2 U_I^{\,*})$$

$$+\frac{V_{an}}{1+U_V}(a^2+aU_V)\frac{I_a^{\ *}}{1+U_I^{\ *}}(a^2+aU_I^{\ *})$$

$$S_{3\phi}=V_{an}I_a^{\ *}\left[\left(\frac{a^2+aU_V}{1+U_V}\right)\left(\frac{a+a^2U_I^{\ *}}{1+U_I^{\ *}}\right)+\left(\frac{a+a^2U_V}{1+U_V}\right)\left(\frac{a^2+aU_I^{\ *}}{1+U_I^{\ *}}\right)+1\right].$$

If a further assumption about the unbalance factor is made, that U_V is negligible compared to the generally much larger U_I, then setting $U_V = 0$ yields,

$$S_{3\phi}=V_{an}I_a^{\ *}\left[\frac{1+aU_I^{\ *}}{1+U_I^{\ *}}+\frac{1+a^2U_I^{\ *}}{1+U_I^{\ *}}+1\right]$$

$$S_{3\phi}=\frac{V_{an}I_a^{\ *}}{1+U_I^{\ *}}\left[2+aU_I^{\ *}+a^2U_I^{\ *}+1+U_I^{\ *}\right]$$

$$S_{3\phi}=3\frac{V_{an}I_a^{\ *}}{1+U_I^{\ *}}. \qquad (3.5)$$

It is reasonable to assume a small U_V, since voltage bus magnitudes are generally determined by low impedance ("stiff") system. Given the assumptions that $U_V \approx 0$, U_I is known, and $V_{an}I_a^{\ *}$ are known, it is thought that the $S_{3\phi}$ value calculated in Equation (3.5) will yield more accurate state estimation results than $S_{3\phi}=V_+I_+^{\ *}$ will alone, when unbalance is present in the system. In the next section, this assumption will be tested in a small test.

3.2 Test cases for observing the effect of the Equation (3.5) adjustment on state estimation

A small test bed has been prepared to study the effect Equation (3.5) can have on state estimation. Equation (3.5) predicts the value of $S_{3\phi}$ given the following assumptions,

- $V_0 = I_0 = 0$
- $V_{an}\, I_a^*$ are known in phasor detail (i.e., magnitude and angle)
- U_I is known in phasor detail at each measurement point
- U_V is negligibly small.

A small three-phase test bed has been created with three buses. The test bed topography is shown in Figure 3.1.

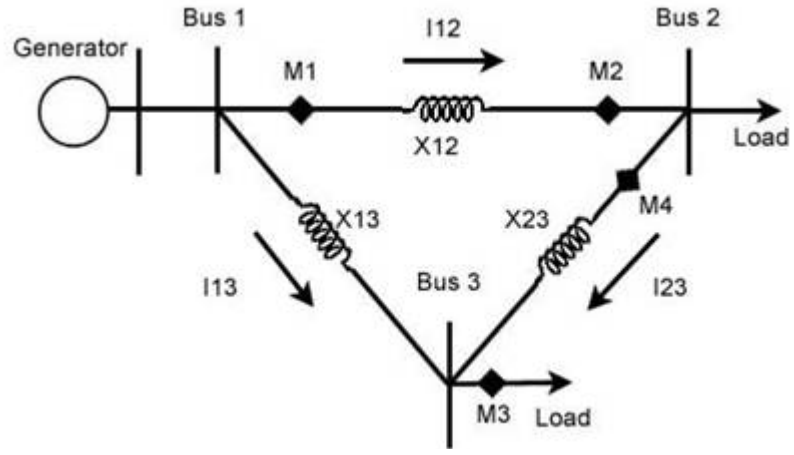

Figure 3.1 The three-bus test bed topology used in Cases 5-8
(lines and loads are three-phase)

The three-bus system shown in Figure 3.1 represents the system in picture detail. The black diamonds show the location of complex power measurement instruments, called M_1, M_2, M_3 and M_4. In this test bed, voltages and line reactance will be assigned and the system parameters will be completely known. Each different test case will be compared to this "perfect measurement" base case as a basis of judging quality.

Unbalance is introduced to the system for test purposes. The most common form of unbalance in a system is unbalanced loads manifesting as unbalanced current [12]. For

the purposes of this test, line parameters have been kept equal on all three-phases phases (representing fully transposed lines), but the voltage phase-neutral values are not balanced. The unbalanced voltage magnitudes were kept within 5% of unity value and voltage angles differed by no more than 5º from their expected, balanced values (0°, -120° and 120° for V_{an}, V_{bn}, and V_{cn}, respectively). Small voltage unbalances will ensure that the U_V is small and therefore negligible, to fit the assumptions. As an example, if

$$V_{an,bn,cn} = \begin{pmatrix} 1.00\angle 0° \\ 1.05\angle -125° \\ 1.00\angle 125° \end{pmatrix},$$

the voltage unbalance factor is 0.0463 $\angle$18.8°.

At this point, consider an example relating to unbalanced three phase conditions. An example denoted in Cases 5-8 is based on the system in Figure 3.1. Unbalanced voltages at V_1, V_2 and V_3 are applied as shown in Table 3.1. The system reactance is shown in Table 3.2. For Cases 5-8, the current unbalance factor is greater than the voltage unbalance (i.e., $|U_I| > |U_V|$). Using the applied unbalanced three-phase voltages in Table 3.1, the resulting currents are listed in Table 3.3. The corresponding active powers and reactive powers are listed in Table 3.4.

Table 3.1 Assigned line-to-neutral base case voltage values for Cases 5-8

	V_1		V_2		V_3	
Phase	$\|V\|$ (p.u. volts)	angle (°)	$\|V\|$ (p.u. volts)	angle (°)	$\|V\|$ (p.u. volts)	angle (°)
an	1	0	1.04	-5	0.98	-3
bn	1	-120	0.98	-115	1.05	-125
cn	1	120	1	125	0.98	125

Table 3.2 Line reactance values for three-phase test bed used in Cases 5-8

	Reactance (p.u. reactance)*
X_{12}	0.01
X_{13}	0.02
X_{23}	0.04

* reactance is the same in phases *a*, *b*, and *c*

Table 3.3 Resulting base case current values for the three-bus test bed used in Cases 5-8

	I_{12}		I_{13}		I_{23}	
Phase	$\|I\|$ (p.u. amps)	angle (°)	$\|I\|$ (p.u. amps)	angle (°)	$\|I\|$ (p.u. amps)	angle (°)
a	9.75	21.68	4.43	-164.47	4.65	-161.12
b	8.86	75.53	5.12	-93.31	4.75	-98.49
c	8.72	-57.5	4.43	-44.47	0.5	35.00

Table 3.4 Three-phase test bed exact power measurements in Cases 5-8

	P (p.u. watts)	*Q* (p.u. vars)
$(S_{3\varphi})_{M1}$	-8.19	-0.85
$(S_{3\varphi})_{M2}$	-8.19	-3.35
$(S_{3\varphi})_{M3}$	6.45	-1.40
$(S_{3\varphi})_{M4}$	3.58	0.75

The values shown in Tables 3.1-3.4 for the system topography shown in Figure 3.1, plus a state estimation algorithm, were programmed and represented in the mathematical software Matlab. The state estimation process used is the WLS method, where the measurement vector *z* is related to the unknown states vector *x* by the matrix *H*,

$$[x] = \left[[H]^T [H] \right]^{-1} [H]^T [z].$$

In the test bed, the measurements are the real and imaginary components of the total three-phase power. Since there are four complex power measurement instruments and each complex power measurement represents a real and imaginary power measurement,

then the vector *x* has dimensions 8x1. The vector of states *z* will be made of the positive sequence bus voltage magnitude and positive sequence bus voltage angle. Under the positive-sequence only assumption, the total complex power can be related to purely positive-sequence values. The vector *z* ignores Bus 1, since that bus has been chosen to be the swing bus and will have a positive-sequence voltage magnitude of $\sqrt{3}$ p.u. at angle 0° with zero negative and zero-sequence components (which is the result of the symmetrical component transformation for a balanced bus voltage where V_a=1∠0° p.u. Therefore, the vector *z* has dimensions 4x1, representing the voltage magnitudes and angles at Buses 2 and 3.

Now the *H* matrix must be constructed to relate total power to the positive sequence voltage value. Since the assumption in the state estimator is only positive sequence values, the power flow calculation can be represented as a single-phase calculation in the positive-sequence system. The per unit value of the perfectly balanced power system will give the following symmetrical components,

$$\begin{bmatrix} V_a \\ V_b \\ V_c \end{bmatrix} = M^{-1} \begin{bmatrix} 1\angle 0° \\ 1\angle -120° \\ 1\angle 120° \end{bmatrix} = \begin{bmatrix} V_+ \\ V_- \\ V_0 \end{bmatrix} = \begin{bmatrix} \sqrt{3} \\ 0 \\ 0 \end{bmatrix}.$$

Because of this, the assumed positive sequence voltage magnitude is $\sqrt{3}$ p.u. under the balanced system assumption. Real power flow in the positive-sequence system would then appear as follows,

$$P_{3\phi} = \frac{|V_{1+}||V_{2+}|}{X_{12}} \sin(\delta_1 - \delta_2).$$

The positive-sequence voltage magnitude is assumed to be $|V_+| \approx \sqrt{3}$. The difference between positive sequence voltage angles is assumed to be small, therefore the value sin(δ_1- δ_2) can be simplified to (δ_1- δ_2), resulting in the following relationship,

$$P_{3\phi} \approx \frac{3}{X_{12}}(\delta_1 - \delta_2).$$

For the imaginary component of the complex power, the following relationship can be used and simplified to construct the rest of the *H* matrix,

$$V_{1+} = \sqrt{3} + \Delta V_1$$
$$V_{2+} = \sqrt{3} + \Delta V_2$$
$$Q_{3\phi} = \frac{|V_{1+}|^2 - |V_1||V_{2+}|\cos(\Delta\delta)}{X} \approx \frac{\sqrt{3}}{X}\left[\Delta V_{1+} - \Delta V_{2+}\right].$$

This is reasonable simplification since the cosine of a small angle difference, such as those between the voltage phases of adjacent buses in a somewhat balanced power system, is very close to 1.0.

Each test case that will be carried out using the above outlined WLS method. The difference between test cases will occur in the manner from which they gather their power measurements. The first set of test cases, called Case 5, will calculate three-phase power given only power measurements from a single-phase. The three-phase total complex power is calculated from the single-phase measurement on the assumption that the power system is completely balanced. The calculation method will appear as follows at each measurement point to calculate the voltage at Buses 2 and 3,

$$S_a \xrightarrow{CALC} S_{3\phi} \xrightarrow{SE} V_+ \xrightarrow{CALC} V_{abc}$$

The resulting states from the state estimation will be compared to the base case for the purposes of quantifying the error. The next test case, namely Case 6, also assumes sin-

gle-phase complex power awareness, but uses Equation (3.5) to calculate a different three-phase power measurement. This test case will be called Case 6 and appear as follows,

$$V_a, I_a, S_a, U_I \xrightarrow{CALC} S_{3\phi} \xrightarrow{SE} V_+ \xrightarrow{CALC} V_{abc}$$

The results of this equation will also be compared to the base case states as well. Case 6 will be compared to Case 5 to see any improvement Equation (3.5) made in the state estimation. Table 3.5, shown later, summarizes these case conditions.

The next set of cases concern single-phase complex power awareness, but the single-phase complex power is calculated from a three-phase power measurement. Although the measurement loses no data through a balanced assumption, the state estimation still assumes positive-sequence only conditions which may introduce error into the results. The next test case will have a measurement vector of single-phase power, which will called Case 7 and be carried by the following outline,

$$\frac{1}{3} S_{3\phi} \xrightarrow{SE} V_{abc}$$

Since the solution to Case 7 will still have some error, Equation (3.5) will be used again to see if there is any improvement. The new case is called Case 8 and will follow this outline,

$$S_a, U_I \xrightarrow{SE} V_+ \xrightarrow{CALC} V_{abc}.$$

These results can be compared to the base case states as well.

Each tests state estimation result will be compared to the perfect measurement state and this result from each test case will be compared to find the most desirable outcome from the test cases. The per-unit voltage magnitudes and the voltage angles for Bus

2 and 3 that result from each test cases state estimation will have the base case values subtracted from them to for the residual, *r*. To compare the residuals from each test case, the 2-norm residual value will be used. The norm calculation is used in mathematics to quantify the size of a vector. If the estimated states were exactly correct, then the 2-norm residual would equal zero. Larger 2-norm residuals will then indicate results that further deviate from perfect values. The 2-norm residual calculation carried out to compare test cases will look like as follows, where *n* is the number of states,

$$|| r ||_2 = || x_{Test} - x_{Perfect} ||_2 = \sqrt{\sum_{k=1}^{n} | r_k |^2} \ .$$

The state estimation calculation for each test case will be run once, without trying to minimize the Jacobian value, as would occur in a more robust WLS state estimator.

Test Cases 5, 6, 7 and 8 will be carried out twice each, once with no error in the measurements, again when a 10% error in the measurements has been introduced. The 10% error cases will be run 1000 times and the average 2-norm residual value from the 1000 runs will be used to compare to the other test results. The tests without error will have the suffix "a," whereas the tests with the 10% error introduced to the measurements will have the suffix "b." A key to the test names is shown in Table 3.5. Complete details on all of the test cases within this thesis are available in Appendix A in Table A.1.

The Cases 5, 6, 7 and 8, with and without error, were calculated with MATLAB software. The resulting state residuals are shown in Table 3.6.

Table 3.5 Key to identify test case names

Test name	ESS calculation method	Measurement error
5a	Single phase power measurement	none
5b	Single phase power measurement	10%
6a	Single phase power awareness with Equation (3.5) adjustment	none
6b	Single phase power awareness with Equation (3.5) adjustment	10%
7a	Single phase power calculated from three-phase power measurement	none
7b	Single phase power calculated from three-phase power measurement	10%
8a	Single phase power calculated from three-phase power measurement with Equation (3.5) adjustment	none
8b	Single phase power calculated from three-phase power measurement with Equation (3.5) adjustment	10%

Table 3.6 The 2-norm residuals of the difference between test states from case 5-8 and the base case states from Table 3.4 values

	Test case names							
	5a	5b	6a	6b	7a	7b	8a	8b
$\|V_2\|$ (p.u. volts)	0.04486	0.04486	0.04366	0.04366	0.04322	0.04322	0.04373	0.04372
δ_2 (rad)	0.17565	0.17569	0.14323	0.14324	0.14254	0.14255	0.14321	0.14322
$\|V_3\|$ (p.u. volts)	0.05945	0.05946	0.05844	0.05844	0.05761	0.05761	0.05770	0.05770
δ_3 (rad)	0.13061	0.13061	0.13917	0.13918	0.13066	0.13069	0.14329	0.14328

Table 3.7 The 2-norm of the residuals between raw state estimates from Cases 5-8 and base case estimates from Table 3.4 values

	$\|\| \hat{x} - x_{exact} \|\|_2$
5a angle (rad)	0.05744
6a angle (rad)	0.03012
5a $\|V\|$ (p.u. volts)	0.02137
6a $\|V\|$ (p.u. volts)	0.01709

	$\|\| \hat{x} - x_{exact} \|\|_2$
7a angles (rad)	0.11917
8a angles (rad)	0.03624
7a $\|V\|$ (p.u. volts)	0.04279
8a $\|V\|$ (p.u. volts)	0.00307

3.3 Observations drawn from test cases

By comparing the state estimated phasor voltage values for Bus 2 and 3 to the base case state values, the impact of Equation (3.5) in state estimation for this test bed becomes apparent. One observation is that the introduced measurement error had little ef-

fect on the test results. The resulting residuals are the same to four decimal places. Because of this, what is said about the results from Case 5a is true for Case 5b. The results in Table 3.6 show that the states calculated in Case 6 were an improvement over the cases calculated in Case 5. To quantify the difference, the percent difference calculation is used,

$$\%difference = \frac{\left|measurement_1 - measurement_2\right|}{\left(\frac{measurement_1 + measurement_2}{2}\right)} * 100\% .$$

The voltage angle residuals from Case 6 had a 2.71% and 1.71% percent difference from the Case 5 voltage angles. The percent difference between the voltage magnitude states between Case 5 and 6 is much more profound, equaling 20.33% and 6.35% (although the Case 5 result for the voltage angle at Bus 3 was closer).

The difference between Cases 6, 7 and 8 are the same to two decimal places and all are an overall improvement compared to the Case 5 results. Case 8, which uses the Case 7 method but with the Equation (3.5) adjustment factor, is very close to the Case 7 results, but offers no improvement for any of the states calculated.

However, the above residuals were calculated from the processed states. That is, the raw states are the positive sequence voltages at Bus 2 and 3 (or the phase *a* voltage at Bus 2 and 3 in the case of Case 7) are then used to calculate the phase-to-neutral voltages at Bus 2 and 3, assuming balance. When the raw residuals are compared to the base case answers and the 2-norm taken, the results seem more promising, as seen in Table 3.7. In each case the state estimator using the Equation (3.5) adjusted power value produced su-

perior results. It is during those results transformation into phase-to-neutral voltages that the results become less impressive.

Since the test bed is small relative to large power systems and the values arbitrary, it is difficult to predict the impact of the Equation (3.5) adjustment factor on a large-scale power system state estimation algorithm. If a larger test bed were used along with actual measurement data, then perhaps a clearer picture of the adjustment factors effect can be gained. A more robust and complete state estimation algorithm may also show an improved picture of the adjustment factors effect. It is also unknown how feasible current unbalance factor measurement throughout a power system is, which will be explored in the next section. However, the adjustment factor may have a worthwhile effect on state estimation results for an unbalanced system that makes SE calculations assuming balanced conditions, with only single-phase awareness.

3.4 Notes on calculating complex unbalance factor without phasor measurements

It should be noted that the complex current unbalance factor, which is used extensively in Chapter 3, is not a commonly metered value. CUF may be easily calculated when three-phase phasor detailed measurements are available, which is increasingly feasible due to the implementation of GPS technologies, however much more common in power utilities are still the traditionally metered values: power flow, injected power, voltage magnitudes and current magnitudes [33]. Fortunately even in a power system where only traditional metered values are reported there are ways to calculate the complex unbalance factor, both VUF and CUF, without new or special equipment. Many of these methods rely on phasor mathematics and only use the per-phase voltage or current mag-

nitudes. Even when the unbalance factor cannot be calculated exactly, it may be worthwhile to calculate an estimate, which will be discussed later in this section.

Represented in the literature there are phasor-detailed voltage unbalance factor calculation methods utilizing the three-phase voltage magnitudes. Often line-to-line voltage magnitude data are available [18], for which there are many methods for calculating the complex VUF. The line to line voltage phasors can be drawn in a triangle configuration. This triangle, with known side-lengths (phasor magnitudes) but unknown angles, contains the angle information of the phasors discerned from trigonometric properties (e.g., the law of cosines). This "voltage triangle" method, where the complex VUF is directly calculated from the line-to-line voltage magnitudes, is presented in detail in [18]. Wagner [32] also shows that the voltage phase angles can be calculated from the three line-to-neutral voltage magnitudes, but only in the absence of a zero-sequence component. Once the voltage phase angles are known along with the magnitudes, the symmetrical components and the unbalance factor can be directly calculated.

Of primary concern for this thesis, however, is the complex current unbalance factor, which is used extensively here. Unlike line-to-line voltage phasors, the current phasors do not always form a closed triangle at any point. However, in ungrounded wye or delta connected systems, such as those in some loads and transformers, the current phasors will sum to zero because without a neutral these currents are subject to Kirchhoff's current law. Presented later in this section is a method for direct calculation of the CUF given the three per-phase current magnitudes, given the presence of an ungrounded delta or wye connection at the point of measurement. For more general cases,

the effects of estimating the phase angles of the current in unbalance factor calculation will now be explored.

Electrical current instrumentation traditionally reports a current magnitude and may or may not report all three phases. Assumptions about phase angles may help estimate CUF. This estimated CUF, when used to calculate the three-phase power at a point, as in Equation 3.5, may improve state estimation in an unbalanced power system. To test the value of estimated current unbalance factor, two sets of estimation criteria were developed.

The first CUF estimation method developed was presumes two current magnitudes are available, called $|I_a|$ and $|I_b|$. This estimation method would be appropriate in a system where single-phase current magnitude sensors are augmented with a single clamp-on CT, or other instrumentation method. The phase *a* current was assigned an angle of zero and the phase *b* current was assigned an angle of 120°, which are the expected values in a balanced system. The assumption being the unbalance is primarily in the current magnitudes, not the angles. The final current phase, I_c, is calculated as follows, assuming an ungrounded wye or delta connection,

$$I_c = -I_b - I_a .$$

These current values were used to calculate the current symmetrical components and then the U_I at each measurement point in the test bed developed in Section 3.2. When compared to the actual complex CUF values from the test bed, the U_I magnitude at any measurement point differed from as little as 4.7% and as much as 99.8% from the actual U_I magnitude. The angle for the estimated U_I differed as little 2.4% and as much as 37.9%

from the actual angle. There is clearly some error from the estimation, but the state estimation results were developed to see if the error is sufficiently negligible. Table 3.8 shows the result from the estimated CUF in the test bed data, where a residual is calculated from the test state estimation results and the actual state values. Much like the result tables in Section 3.3, Cases 6 and 8 use the $S_{3\varphi}$ calculation from Equation 3.5 to improve state estimation (only with the estimated U_I used in the $S_{3\varphi}$ calculation this time). Case 5 has the states calculated from single-phase data under a balanced operation assumption and Case 8 is still state estimation calculated from three-phase data under a balanced system assumption. Case 6 has a smaller residual compared to Case 5 and Case 8 has a smaller residual compared to Case 7, signifying an improvement when Equation 3.5 is employed, even with the estimated U_I value. Comparing the 2-norm residuals from Table 3.8 to that of the "exact" U_I case in Table 3.7 reveals that while both methods offer an improvement, that the "exact" U_I case has superior results, which is to be expected. However, the differences are small and despite the sometimes large difference between the calculated U_I and the true U_I, the results are still superior compared to the states estimated under the balanced operation assumption alone.

Table 3.8 Normalized state estimate residuals from the three-phase test bed utilizing the two-magnitude, estimated U_I method, using Cases 5-8 system data

	$\|\| \hat{x} - x_{exact} \|\|_2$		$\|\| \hat{x} - x_{exact} \|\|_2$
5a angles (rad)	0.05744	7a angles (rad)	0.11917
6a angles (rad)	0.03098	8a angles (rad)	0.04860
5a $\|V\|$ (p.u. volts)	0.02137	7a $\|V\|$ (p.u. volts)	0.04279
6a $\|V\|$ (p.u. volts)	0.01263	8a $\|V\|$ (p.u. volts)	0.01184

The assumption-based CUF estimation will now be studied again, but this time with all three current magnitudes presumed known, rather than only two as was used before. This could represent a situation where three-phase current magnitudes are metered or single-phase current instruments have been augmented. In a similar fashion to the previous test, the phase *a* current is assigned an angle of zero, the phase *b* current is assigned an angle of 120°, and the phase *c* current has known magnitude and satisfies the following,

$$I_c = -I_b - I_a .$$

This method contains additional information over the last assumption-based method (the phase *c* magnitude is known). These estimated CUF values were again calculated from the Section 3.2 test bed and compared to the actual U_I values. The U_I angles differed by as little as 0.3% to as much as 80.2% from the actual. The U_I magnitudes differed by as little as 23.72% to as much as a stunning 649.17%. Again the assumption-based U_I are used in the Equation 3.5 calculation, resulting in the 2-norm residuals of the states compared to the base case values shown in Table 3.9.

Table 3.9 Normalized state estimate residuals from the three-phase test bed utilizing the three-magnitude, estimated U_I method, using Cases 5-8 system data

	$\|\hat{x} - x_{real}\|_2$		$\|\hat{x} - x_{real}\|_2$
5a angles (rad)	0.05744	7a angles (rad)	0.11917
6a angles (rad)	0.04728	8a angles (rad)	0.04860
5a $\|V\|$ (p.u. volts)	0.02137	7a $\|V\|$ (p.u. volts)	0.04279
6a $\|V\|$ (p.u. volts)	0.01416	8a $\|V\|$ (p.u. volts)	0.00845

Despite the added information, the resulting states offer results better and worse than those of the $|I_a|$ and $|I_b|$ method in Table 3.8. This may be due to the singularly large estimated U_I magnitude error in the test data. What is clear is that the assumption based U_I calculation method paired with the Equation 3.5 method may offer an advantage for calculating states in an unbalanced three-phase system.

While the Table 3.8 and 3.9 results show the estimated U_I method can give superior results to the balanced operation assumption alone, the Equation 3.5 method for improving state estimation parameters is designed for the exact U_I value. Under special circumstances, the CUF can be calculated from the three-phase current magnitudes in a similar manner to the VUF calculation methods presented earlier in this section. When the three-phase currents sum to zero (or are assumed to do so), the resulting phasors can be drawn in a closed triangle (see Figure 3.2). This is the case at any ungrounded wye or delta connection.

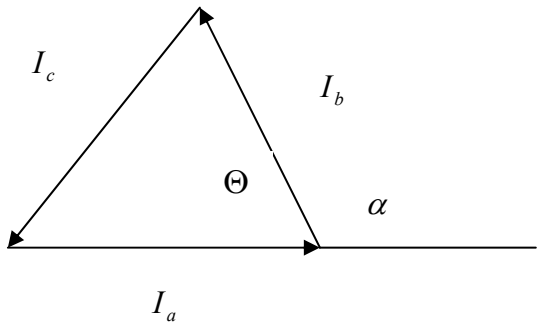

Figure 3.2 Three-phase current phasors that sum to zero

Through the law of cosines the angle between phase *a* and *b* can be described as follows,

$$\cos\theta = \frac{|I_c|^2 - |I_a|^2 - |I_b|^2}{-2|I_a||I_b|}.$$

The angle complimenting θ in Figure 3.1 is called α and since cos α=-cos θ,

$$\cos\alpha = \frac{|I_c|^2 - |I_a|^2 - |I_b|^2}{2|I_a||I_b|}. \tag{3.6}$$

The numerator and denominator in Equation 3.6 can be said to describe a triangle, shown in Figure 3.3.

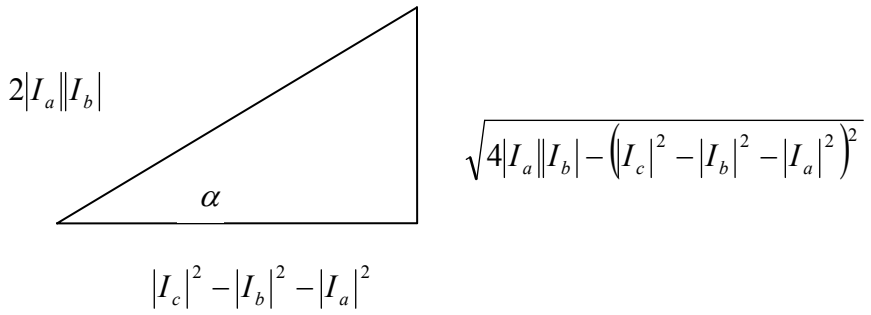

Figure 3.3 Right triangle from angle α and law of cosines relationship

Using this information and knowledge of the three-phase current magnitudes, the complex current unbalance factor can be derived. The first step is setting the phase *a* current as the reference current with angle zero,

$$I_a = |I_a| \angle 0°.$$

The angle α derived earlier describes the relative angle between phase *a* and phase *b*, whereas the phase *b* current can be described in rectangular notation as,

$$I_b = |I_b|(\cos\alpha + j\sin\alpha). \tag{3.7}$$

The cosα portion of Equation 3.7 is described in Equation 3.6. The sinα portion of Equation 3.7 may be derived from the right triangle presented in Figure 3.3, which is as follows,

$$\sin\alpha = \frac{\sqrt{4\,|I_a|^2|I_b|^2 - (|I_c|^2 - |I_a|^2 - |I_b|^2)^2}}{2\,|I_a||I_b|}.$$

The final calculation for I_b is as follows, where the sign for the square root portion is arbitrarily chosen to be negative to reflect the tendency for positive sequence over negative sequence in a power system,

$$I_b = \frac{|I_c|^2 - |I_a|^2 - |I_b|^2}{2\,|I_a||I_b|} - j\frac{\sqrt{4\,|I_a|^2|I_b|^2 - (|I_c|^2 - |I_a|^2 - |I_b|^2)^2}}{2\,|I_a||I_b|}.$$

Since the current phasors form add up to zero, the *c* phase current is simply calculated as,

$$I_c = -I_b - I_a.$$

Using the three current phases described in phasor detail, the symmetrical components are calculated, which is used to find the complex current unbalance factor. Multiplying by the symmetrical component transformation matrix, with the symmetrical transformation matrix coefficient ignored since it will divide out in the unbalance factor equation, the following symmetrical components result,

$$M = \pm\frac{\sqrt{4\,|I_a|^2|I_b|^2 - (|I_c|^2 - |I_a|^2 - |I_b|^2)^2}}{2\,|I_a||I_b|}$$

$$\alpha = 1\angle 120° = -\frac{1}{2} + j\frac{\sqrt{3}}{2}$$

$$I_+ = I_a + \alpha I_b + \alpha^2 I_c$$

$$I_{+} = \frac{3}{2}|I_a| \pm \left(\sqrt{3}\right)M + j\left(\frac{\sqrt{3}\left(|I_c|^2 - |I_b|^2\right)}{2|I_a|}\right)$$

$$I_{-} = I_a + \alpha^2 I_b + \alpha I_c$$

$$I_{-} = \frac{3}{2}|I_a| \mp \left(\sqrt{3}\right)M + j\left(\frac{\sqrt{3}\left(|I_b|^2 - |I_c|^2\right)}{2|I_a|}\right).$$

$$U_I = \frac{I_{-}}{I_{+}} = \frac{\frac{3}{2}|I_a| \pm \left(\sqrt{3}\right)M + j\left(\frac{\sqrt{3}\left(|I_b|^2 - |I_c|^2\right)}{2|I_a|}\right)}{\frac{3}{2}|I_a| \mp \left(\sqrt{3}\right)M + j\left(\frac{\sqrt{3}\left(|I_c|^2 - |I_b|^2\right)}{2|I_a|}\right)} \tag{3.8}$$

Equation 3.8 is a direct calculation of U_I from current magnitudes, but can be further simplified. If the current magnitudes are normalized to I_a by dividing all of the magnitudes by $|I_a|$, then $|I_a|$ becomes unity. The normalized current magnitudes will have the letter "n" as a suffix after the phase identification and should not be confused with the line-to-neutral notation, which only have common usage in reference to voltages. The result is the following set of equations,

$$|I_{bn}| = \frac{|I_b|}{|I_a|}$$

$$|I_{cn}| = \frac{|I_c|}{|I_a|}$$

$$U_I = \frac{I_{-}}{I_{+}} = \frac{3|I_a| \pm \left(\sqrt{3}\right)\sqrt{4|I_b|^2 - \left(|I_c|^2 - |I_b|^2 - 1\right)^2} + j\left(\sqrt{3}\left(|I_b|^2 - |I_c|^2\right)\right)}{3|I_a| \mp \left(\sqrt{3}\right)\sqrt{4|I_b|^2 - \left(|I_c|^2 - |I_b|^2 - 1\right)^2} + j\left(\sqrt{3}\left(|I_c|^2 - |I_b|^2\right)\right)} \tag{3.9}$$

Due to the square root calculation for the *M* value, there is an ambiguity of sign. Through experimentation, it has been shown that for predominately positive sequence systems, where the phase *b* current has a negative angle in reference to phase *a*, the *M* in the numerator is negative and the *M* in the denominator is negative. When phase *b* has a positive angle in reference to phase *a*, then the *M* in the numerator is positive and the *M* in the denominator is negative. Since the positive sequence current is often larger than the negative sequence current, even in unbalance, the positive sequence answer for the unbalance factor calculation may be assumed. The following equation illustrates this value,

$$U_I = \frac{I_-}{I_+} = \frac{3|I_a| - \left(\sqrt{3}\right)\sqrt{4|I_b|^2 - \left(|I_c|^2 - |I_b|^2 - 1\right)^2} + j\left(\sqrt{3}\left(|I_b|^2 - |I_c|^2\right)\right)}{3|I_a| + \left(\sqrt{3}\right)\sqrt{4|I_b|^2 - \left(|I_c|^2 - |I_b|^2 - 1\right)^2} + j\left(\sqrt{3}\left(|I_c|^2 - |I_b|^2\right)\right)}. \qquad (3.10)$$

Equation 3.10 allows exact calculation of the complex CUF, if the current I_a is taken as the reference value (angle is zero). In the absence of metering of the U_I value or three-phase current phasor measurements, this can make the Equation 3.5 three-phase power calculation possible and improve state estimation in an unbalanced system.

3.5 Summary of results

The formula derived earlier in this section, called Equation 3.5, makes it possible to calculate three-phase complex power from a single phase complex power measurement and the complex current unbalance factor, if voltage unbalance and negative sequence information are both negligible. This has many advantages in state estimation, including making three-phase measurements possible from single-phase measurements, when the

complex CUF is known. Many situations where Equation 3.5 might improve measurements were modeled and studied. The question of calculating the complex current unbalance factor where direct measurements are not available was also tested, as well as the viability of estimating the complex CUF.

Test Cases 5-8 were conducted to show how use of Equation 3.5 on system measurements may improve state estimation results for a hypothetical 3 bus power system. In general, Cases 5-8 operate on an assumption of balanced conditions and perform WLS under that assumption. The details of Cases 5-8 can be found in Section 3.2 and the details of the Cases 5-8 are outlined in Table 3.5. The results of these Cases are shown in tables 3.6 and 3.7, where the 2-norm of the first iteration state estimations residuals is compared. In general, Equation 3.5 yielded improved first iteration state estimation results compared to similar cases that did not use Equation 3.5.

In Section 3.4, the viability of estimating the complex current unbalance factor was examined and calculations similar to Cases 5-8 were performed, utilizing the three-bus test bed. The complex current unbalance factor estimation criteria used created CUFs that were sometimes close to the exact value and sometimes very much different. Despite the mixed results in estimating complex CUF, Cases 5-8 were run again and again showed improved first iteration state estimation results under the testing criteria, however the improvement less compared to when the exact complex current unbalance factor was known.

Next a method for directly calculating the current unbalance factor from three-phase current magnitude measurements was presented. The method requires three-phase current magnitude measurements and must be at an ungrounded delta or wye connection.

CHAPTER 4 LINEAR PREDICTION METHODS FOR NON-SIMULTANEOUS MEASUREMENT CORRECTION TO IMPROVE STATE ESTIMATION

4.1 Non-simultaneous measurements

State estimation relies on measurement inputs which may have no time stamp. Because of this, measurements with time delay could be erroneously accepted as simultaneous (no delay) by state estimation algorithms. The measurement may be flagged as being in error; however, the error may be identified as measurement error. Delayed measurements in a power system are a real concern and can be caused by a variety of sources. Communication systems can be a source of measurement delay, for instance if there is not have enough bandwidth to accept all measurements in a timely fashion. Instruments may also operate on delayed clocks, although with GPS technology to synchronize time signals this to may be increasingly less common in modern systems. More prevalent are time delays caused by the cooperation between separate but interconnected power entities, where information is exchanged, possibly through a central power pool. Power entities may be inclined to incorporate interconnected power system measurement and state information, but differences in communication, timing, and other operational issues can manifest themselves in a delay of a few seconds for real time measurements and a delay of as much as 60 minutes for state estimation results [23], [29]. Furthermore, these delays may be of unpredictable occurrence and length. Some instruments, most notably phasor measurement units (PMUs), offer time stamping on their readings. A PMU is a GPS based instrument which utilizes four or more signals from GPS satellites to obtain an absolute time. Using absolute time as a time stamp, the PMU can fit a “best”

sine wave to a voltage or current measurement and thereby make a phasor measurement. Until PMU use becomes more widespread, time stamping may be an unrealistic solution to measurement delay problems. Even when time stamps are available, interpolation software may be needed to correlate (match) measurements.

Many stochastic prediction techniques exist in the literature to improve delayed measurements, including auto regressive-moving average techniques, Winter's multiplicative seasonal model, and Kalman filtering techniques [22-23], [29], [35]. These algorithms may rely on measurements with known latency delay lengths; measurements with a known delay probability (i.e., a known or assumed statistical model for latency); measurements with a known or assumed dynamic model such as forcing functions. The effort here is to explore the use of a simpler linear process that operates with less required information to improve delayed measurements and the resulting state estimation.

4.2 Linear measurement prediction

A linear, autoregressive process is considered for signal prediction, which will take the general form,

$$\underset{mxn}{z}\ \underset{nx1}{A} = \underset{mx1}{\hat{z}}. \tag{4.1}$$

A measurement vector is defined as n consecutive sampling time periods in length (the vector z in (4.1)). The vector z is multiplied by a relation matrix A to form a measurement prediction $\hat{z}$, at time t. This is accomplished using the algorithm presented in Figure 4.1.

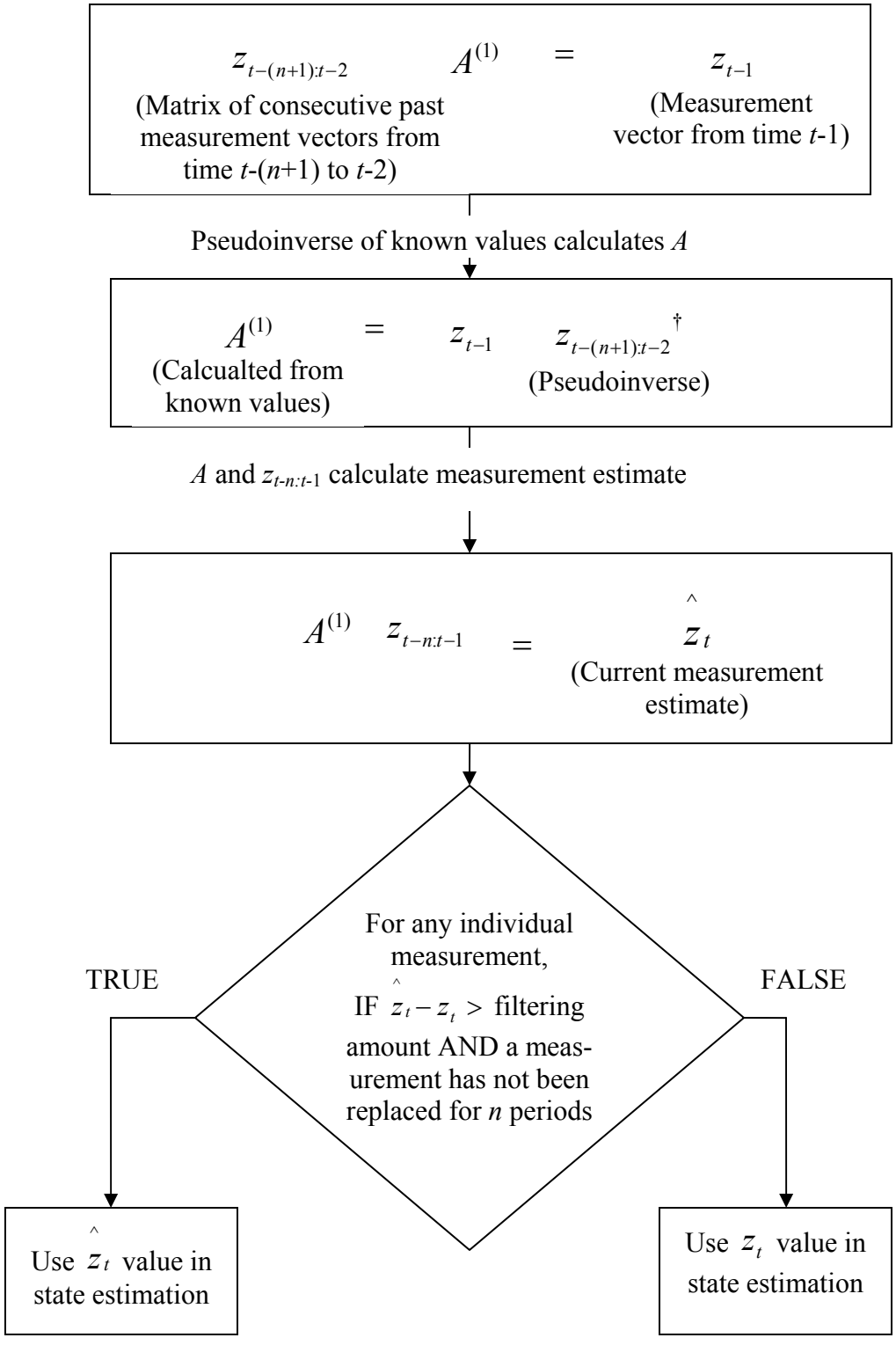

Figure 4.1 The linear measurement prediction model algorithm

As shown in Figure 4.1, a value of A is calculated from a set of recent, consecutive measurements in memory, where A is calculated by multiplying the measurement vector from time t-1 to the pseudo-inverse of the matrix of past measurement vectors from time t-n+1 to t-2. This A is used as an estimate for the A which relates the measurements from time t-n to t-1 to the measurement at time t. This method makes very accurate predictions of a signal (assuming noiseless measurements) if:

- The sampling time period used to take measurements is frequent relative to the rate of change of the signal being measured.
- The past number of measurements in memory (n+1) is sufficiently large (in practice, at least 3 or more for good predictions, see the test cases for more detail).

These are reasonable assumptions for a power system under normal conditions in the absence of high speed dynamics (so-called "stable" conditions). Power system metering may sample several times a second, therefore during normal operation the rate of change of typical measurements, like real and reactive power, will likely be small compared to the possible measurement sampling rate. Note that the term "stable" does not refer to system stability in this case; rather, the tern is used to describe system dynamics that are not highly varying.

Intuitively, large amounts of measurements kept in memory may yield better estimation results compared to smaller numbers of measurements. Larger blocks of past measurements will add more information to the linear prediction model and, when delayed measurements are present, allow for more non-delayed measurements to influence the prediction model. This assumption will be tested later in this section.

However, a problem with delayed measurements in a power system is that they are not perfect measurements. The appearance of a randomly delayed measurement in a continuous set of data is presented in Figure 4.2. The delayed measurements used in the linear prediction model as presented in Figure 4.1 may add error to the prediction result. The challenge then is to find ways to optimize this prediction model, such that the predictions are appreciably better than the delayed measurement signal alone. Making the linear prediction algorithm give superior results has the following challenges:

- Have enough past measurements in memory to allow for better predictions.
- Not having as many past measurements in memory as to cause storage issues or burdensome amounts of additional calculation.
- Having a large number of measurements compared to the rate of change in the measurement signal.
- Creating a set of past measurements accurate enough to make usable predictions.

The logical next step would be to use the corrected measurement signal produced by the linear algorithm and use this corrected value in the next step of the prediction method, however this can be problematic. Use of corrected measurements in the linear prediction method can result in large prediction errors relative to the uncorrected delayed signal, which in turn introduces even greater error into the prediction algorithm. Examples of delayed measurement signals and the "spikes" this information can cause in the prediction output are presented in Figure 4.3. When these errors, large relative to the de-

layed measurements, are used in the signal prediction estimator, the error compounds and the prediction error can grow several orders of magnitude. Because of this, the delayed measurement signal is selected to be used in the linear prediction algorithm since it is the least problematic of the choice of signals. The challenge then becomes one of finding a way to improve the linear algorithm given the delayed input.

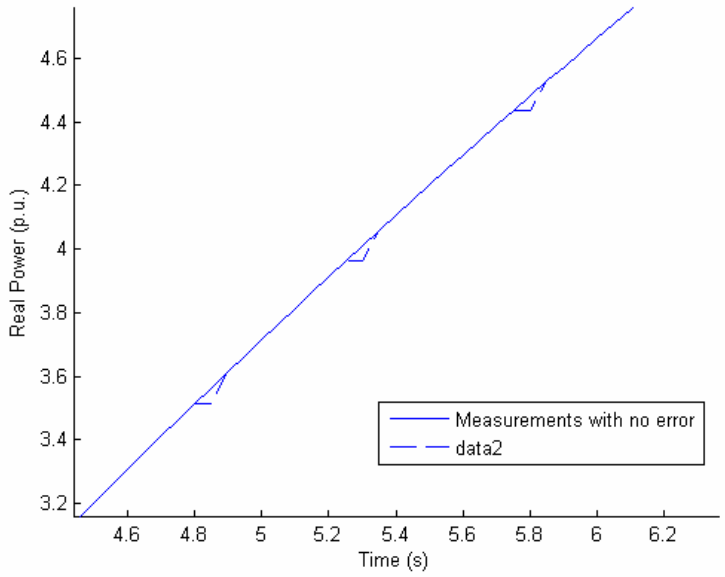

Figure 4.2 An example of a randomly delayed measurement signal with sampling period 0.5 s and P measured in per unit, from Case 9a

The solution found to the "prediction spikes" was to avoid making a measurement correction as long as a suspected delayed measurement is in memory. In short, if *n* previous time periods are in memory, then only one delayed measurement replacement can be performed during *n* time periods.

This prediction improvement strategy adds the following concerns to the linear prediction method:

- The previous measurements in memory *n* cannot be too large; otherwise the correction method is hardly used.
- The replacement algorithm will not correct every delayed measurement, but should produce an improved set of measurements for state estimation.
- Since only one measurement replacement per *n* time periods is performed, the probability of delayed measurements should be small over this time period to avoid not correcting a large amount of delayed measurements.

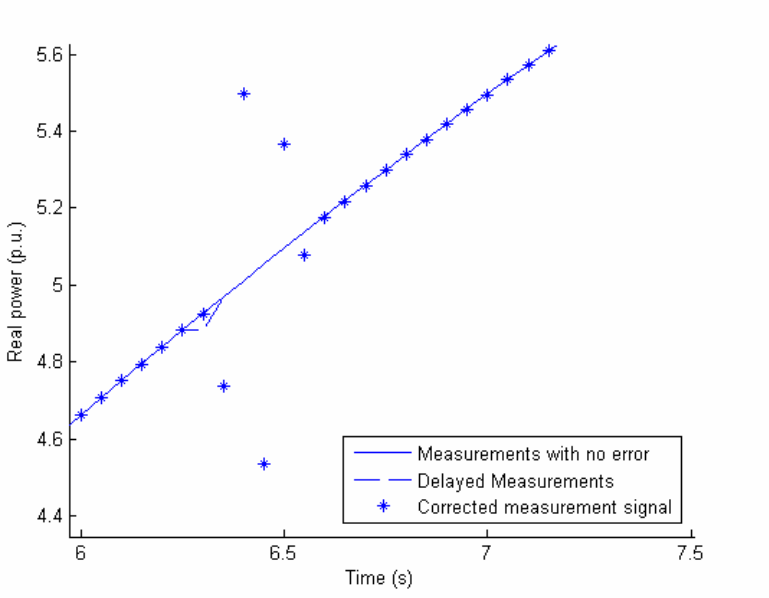

Figure 4.3 An example of the randomly delayed measurements effect on the linear prediction algorithm, from Test Case 9a

With this new improvement to the algorithm shown in Figure 4.1, the testing phase was conducted.

4.3 Test case to find optimal linear prediction method

The general linear signal prediction method was used on test data to find what the optimal linear prediction algorithm. A test bed power system was created in Matlab, with sample code provided in Appendix B. The test power system is an invented five bus power system, with seven instruments that measured real power flow. No $|V|$ prediction was attempted. The power flow equation used was as follows,

$$P = \frac{|V_1||V_2|}{X}\sin(\delta_1 - \delta_2) \approx \frac{1}{X}(\delta_1 - \delta_2).$$

The familiar weighted least squares state estimation equations was compiled where the state vector x was composed of the bus voltage angles, the measurement vector z was composed of real power measurements, and the relationship matrix H was composed of $1/X$ values relative to the above power flow equation, shown here,

$$z = Hx.$$

The five bus, seven instrument power system is shown in Figure 4.4. The topography was invented, as were the line reactances. Power measurements are invented, where each instrument was assigned a separate non-repeating sinusoid value for its power reading, with similar bandwidth. Power and reactance values are in per unit. Bus angles are in radians.

Several different test cases were conducted to study the linear measurement predictions benefit in different systems. All of the test cases had this in common: each measurement had a 5% chance of being delayed by one time period. The proposed algorithm shown in Figure 4.1 allows for several different variables, with each combination representing a test case: the A matrix was either calculated once for the testing period (Cases 9, 10, 12 and 13) or continuously updated (Cases 11 and 14), the A matrix was

calculated from randomly delayed measurements (Cases 9 and 11) or from "perfect" measurements (Cases 10 and 12), from noiseless signals (Cases with suffix "a") and signals with a random measurement error of up to 10% the real value (Cases with suffix "b"), and finally cases with power signals of relatively high bandwidth (1.5 radians/time-period, Cases 12-14) to cases with relatively low bandwidth (0.15 radians/time-period, Cases 9-11). The differences between the different cases are outlined in Table 4.1 and in Appendix A.

The different test cases were performed to study the performance of the linear test method. One difficulty which immediately became apparent was the choice of signal for calculating the *A* matrix: the corrected signal, or the uncorrected signal with random delays. It was found that using the delayed measurements in the predication algorithm would cause poor predictions. Measurements without delay kept in memory would produce good predictions, but as soon as a delayed measurement was introduced into memory it would cause an error in the prediction, often greater than the error of a delayed measurement. This is illustrated in Figures 4.2 and Figure 4.3.

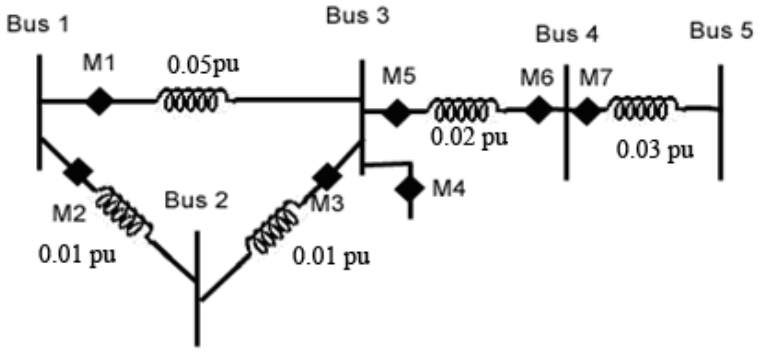

Figure 4.4 The five bus test bed for Cases 9-14

Table 4.1 Identities of test Case 9-14

Case	*A* matrix	Measurement error	Signal bandwidth
9a	calculated once (delayed)	None	0.15 radians/time period
9b	"	10%	"
10a	calculated once (no delay)	None	"
10b	"	10%	"
11a	updated continuously	None	"
11b	"	10%	"
12a	calculated once (delayed)	None	1.5 radians/time period
12b	"	10%	"
13a	calculated once (no delay)	None	"
13b	"	10%	"
14a	updated continuously	None	"
14b	"	10%	"

Several sets of criteria were used to rank the different test case results. One was the minimum length *n* of the past measurement matrix needed to produce measurement predictions that are better than the delayed measurements most of the time. Another calculation performed was the 2-norm residual of the delayed measurements subtracted from the real measurements, and the 2-norm of the corrected delayed measurements subtracted from the real measurements. The linear prediction method residuals were calculated at an *n* value that produced more prediction values closer to the exact signal than delayed signal values closer to the actual signal. The results are shown in Table 4.2.

Analyzing the results in Table 4.2 shows the strengths and weaknesses of the linear prediction method.

- A 2-norm residual closer to zero is deemed the more desirable result, since the test results were closer to the actual values. For instance, the test runs with the "b" suffix, where random 10% noise is added, are always less desirable than the noiseless solutions.

- Cases with a higher change in signal per sampling time period (Cases 12-14) gives results less desirable than those in the low change cases (Case 9-11).
- Cases where the *A* relationship matrix is not continually calculated (Cases 9-10, 12-13) also give improved results compared to continually updated cases (Case 11, 14).
- When *A* is calculated once, it is advantageous to use measurements without delay, such as in Cases 10 and 13. This may be done during a period of low latency to "tune" the algorithm.

Table 4.2 Results for test Cases 9-14

Case	Min size *n*	Size *n* used in test	2-norm of measurement residual		2-norm of state residual	
			Delayed signal	Corrected signal	Delayed signal	Corrected signal
9a	5>	5	0.1829	0.1539	8.603e-4	6.178e-4
9b	10>	10	3.6675	3.4935	.06794	.06757
10a	10>	10	0.1453	0.0852	7.9785e-4	6.5072e-4
10b	10	10	3.7674	3.8874	.0667	.0664
11a	5-17	10	0.1120	0.1265	8.6173e-4	5.6278e-4
11b	15>	15	3.5170	13.4748	0.0650	0.2021
12a	3-13	3	0.8536	1.2795	0.0137	0.0130
12b	60>	60	2.9117	50.4776	0.0543	0.4923
13a	3-15	3	0.8572	0.5729	0.0123	0.0063
13b	50>	50	2.9394	45.0016	0.0562	0.3966
14a	6-8	7	0.9306	1.3935	0.0146	0.0156
14b	30>	30	3.2545	41.6380	0.0524	0.3548

Many things about the linear prediction method can be inferred from these generalized results. For instance, *A* should not be continually updated, since it is computationally more expensive and offers no discernable advantage. Also, low measurement noise is preferable. The argument is made for the value of pre-estimation noise filtering.

When only 10% noise is added to the test bed, the linear algorithm cannot offer improved results, probably due to larger “prediction spikes” like those shown in Figure 4.3.

Power systems with a low probability of delayed measurements per time period during times of low system change may derive a benefit from this linear measurement correction algorithm. However, noisy, chaotic systems may not. Power systems where this prediction algorithm is not appropriate may instead benefit from the stochastic correction algorithms presented in the literature that require a more in-depth study of the cause and model of delay.

CHAPTER 5 CONCLUSIONS AND RECOMMENDATIONS

5.1 Conclusions

The main conclusions of this work are:

- It is possible to correct the measurement error associated with reactance in-between the CT and PT component of a power measurement from knowing the non-collocated power measurement, a local voltage magnitude, and the reactance. This is a software solution that avoids hardware reinstallation and may have a positive effect of state estimation results by lowering estimate error and, more dramatically, lowering state estimate variance.

- State estimators that incorporate three-phase power flow may operate under a balanced system assumption when unbalanced conditions. A more accurate three-phase power calculation may be calculated from single-phase measurements and the complex current unbalance factor, resulting in improved state estimation output. Methods for estimating or directly calculating the complex current unbalance factor are also presented.

- A linear signal prediction algorithm is presented which may have a positive effect on power system state estimation in the presence of measurement latency. The presented algorithm has the advantage of being less complex than existing delayed measurement correcting algorithms presented in the literature.

5.2 Recommendations

Recommendations for future work include:

- Correcting non-collocated power measurements with different known values (this paper assumes a local $|V|$ is known as well as accurate reactance information).
- Considering the iterating WLS SE case for each test case.
- Calculating better three-phase power flow with the complex current unbalance factor to improve states estimation in unbalanced conditions may be expanded to include the following:
    - Finding instrumentation needed to calculate the complex CUF exactly.
    - Cases for when the complex voltage unbalance factor cannot be assumed to be zero.
    - Cases that include zero-sequence unbalance in the power system.
- For non-simultaneous measurement cases:
    - Implement and test Kalman Filter solutions
    - Compare findings to real data
    - Consider cases with relatively long measurement delays
    - Include Q and $|V|$ in the state estimation results.

REFERENCES

[1] A. P. Sakis Meliopoulos, “State estimation for mega-RTOs,” 2002 IEEE Power Engineering Society Summer Meeting, v. 3, July 21-25, 2002, pp. 1698–1703

[2] F. C. Schweppe, J. Wildes, and D. B. Rom, “Power system static state estimation,” Part I, II, III, IEEE Transactions on Power Apparatus and Systems, v. PAS-89, No. 1, Jan. 1970, pp. 120-35.

[3] R. E. Kalman, “A new approach to linear filtering and prediction problems,” Journal of Basic Engineering (ASME), 82D, March 1960, pp. 35-45.

[4] A. H. Vuong, S. Lefebvre, X. D. Do, “Detection and identification of topological errors from real-time measurements reconciliation,” 2002 IEEE Power Engineering Society Winter Meeting, v. 1, Jan. 27-31, 2002, pp. 228-233.

[5] J. C. S. Souza, A. M. Leite da Silva, A. P. Alves da Silva, “Data debugging for real-time power system monitoring based on pattern analysis,” IEEE Transactions on Power Systems, v. 11, Aug. 1996, pp. 1592-1599.

[6] K. A. Clements, P. W. Davis, “Detection and identification of topology errors in electric power systems,” IEEE Transactions on Power Systems, v. 3, Nov. 1988, pp. 1748-1753.

[7] A. Simões Costa, J. A. Leão “Identification of topology errors in power system state estimation,” IEEE Transactions on Power Systems, v. 8, Nov. 1993, pp. 1531-1538

[8] L. Mili, G. Steeno, F. Dobraca, D. French “A robust estimation method for topology error identification,” IEEE Transactions on Power Systems, v. 14, Nov. 1999, pp. 1469-1476.

[9] F. F. Wu, W-H E. Liu, "Detection of topology errors by state estimation," IEEE Transactions on Power Systems, v. 4, Feb. 1989, pp.176-183.

[10] W.-H. E. Liu, S.-L. Lim, "Parameter error identification in power system state estimation," IEEE Transactions on Power Systems, v. 4, Feb. 1989, pp. 176-183.

[11] A.P.S. Meliopoulos, F. Zhang, "Multiphase power flow and state estimation for power distribution systems," IEEE Transactions on Power Systems, v. 11, May 1996, pp. 939-946.

[12] C. W. Hansen, A. S. Debs, "Power system state estimation using three-phase models," IEEE Transactions on Power Systems, v. 10, May 1995, pp. 818-824.

[13] S. Zhong, A. Abur, "Effects of non-transposed lines and unbalanced loads on state estimation," 2002 IEEE Power Engineering Society Winter Meeting, v. 2, Jan. 27-31, 2002, pp. 975-979.

[14] J. Zhu, D. Hwang, et al., "Real time congestion monitoring and management of power systems," 2005 IEEE/PES Transmission and Distribution Conference and Exhibition: Asia and Pacific, Aug. 15-18, 2005, pp. 1-5.

[15] S.-G. Jeong, "Representing line voltage unbalance," Conference Record of the Industry Applications Conference, 37th IAS Annual Meeting, v. 3, Oct. 13-18, 2002, pp. 1724-1732.

[16] Y.-J. Wang, "Analysis of effects of three-phase voltage unbalance on induction motors with emphasis on the angle of the complex voltage unbalance factor," IEEE Power Engineering Society Winter Meeting 2002, v. 2, Jan. 27-31, 2002, pp. 1235.

[17] A. J. Wood and B.F. Wollenberg, Power Generation, Operation and Control, New York: John Wiley & Sons, Inc., 1996.

[18] S.-G. Jeong, "Representing line voltage unbalance," Conference Record of the Industry Applications Conference, 2002. v. 3, Oct. 2002, pp. 1724-1732.

[19] T.-H. Chen, "Evaluation of line loss under load unbalance using the complex unbalance factor," IEE Proceedings: Generation, Transmission, and Distribution, v. 142, March 1995, pp.173-178.

[20] Y.-J. Wang, "Analysis of effects of three-phase unbalance on induction motors with emphasis on the angle of the complex voltage unbalance factor," IEEE Transactions on Energy Conversion, v. 16, Sept. 2001, pp. 270-275.

[21] R. E. Wilson, "PMUs [phasor measurement units]," IEEE Potentials, v. 13, Apr. 1994, pp. 26-28.

[22] R. C. Leou, C. N. Lu, "Adjustment of the external network's measurements and its effect on the power mismatch analysis," Conference record of the 1999 IEEE Industry Applications Conference, v. 3, Oct. 3-7, 1999, pp. 2072-2076.

[23] C.-L. Su, C.-N. Lu, "Interconnected network state estimation using randomly delayed measurements," IEEE Transactions on Power Systems, v. 16, Nov, 2001, pp. 870-878.

[24] IEEE Standard for Synchophasors of Power Systems, IEEE 1344-1995.

[25] K. E. Martin, "Precise timing in electric power systems," Proceedings for the 1993 IEEE International frequency Control Symposium, June 2-4, 1993, pp. 15-22.

[26] B. Xu, A. Abur, "Observability analysis and measurement placement for systems with PMUs," IEEE PES Power Systems Conference and Exposition, v. 2, 10-13 Oct, 2004, pp. 943-946.

[27] X. Dongjiw, H. Renmu, W. Peng, X. Tao, "Comparison of several PMU placement algorithms for state estimation," Eights IEEE International Conference on Developments in Power System Protection, v. 1, April 5-8, 2004, pp. 32-35.

[28] R. Živanović, C. Cairns, "Implementation of PMU technology in state estimation: an overview," IEEE 4th AFRICON, v. 2, Sept, 24-27, 1996, pp. 1006-1011.

[29] A. P. S. Meliopoulos, B. Fardanesh, S. Zelingher, "Power system state estimation: modeling error effects and impact on system operation," Proceedings of the 34th Annual Hawaii International Conference on System Sciences, 2001, Jan. 3-6, 2001, pp. 682-690.

[30] N. P. Tobin, "Measuring line currents remotely," IEEE Transmission and Distribution Conference and Exposition, 2001, v. 1, Oct. 2001, pp. 107-112.

[31] J. A. L. Ghijselen, A. P. M. van der Bossche, "Exact voltage unbalance assessment without phase measurements," IEEE Transactions on Power Systems, v. 20, Feb. 2005, pp. 519-520.

[32] C. F. Wagner, R. D. Evans, Symmetrical Components, Malabar, Florida: Robert E. Krieger Publishing Company, 1986.

[33] L. Zhao, A. Abur, "Multiarea state estimation using synchronized phasor measurements," IEEE Transactions on Power, v.20, May 2005, pp. 611-617.

[34] R. G. Brown, Introduction to Random Signal Analysis and Kalman Filtering, New York City, New York: John Wiley & Sons, Inc., 1983.

[35] J. M. Parr, C. L. Philips, "State estimation from retarded measurements," IEEE Southeastcon '89 proceedings, v.3, 9-12 April, 1989, pp. 1275-1280.

[36] F. C. Schweppe, Uncertain Dynamic Systems, Wiley, New York, 1965.

[37] A. Monticelli, State Estimation in Electric Power Systems: A Generalized Approach, Kluwer International Series in Engineering and Computer Science, 1999.

[38] G. Heydt, Computer Analysis Methods for Power Systems, Stars in a Circle Publications, Scottsdale AZ, 1995.

[39] L. Weinberg, P. Slepian, "Realizability conditions on n-port networks," IRE Transactions on Circuit Theory, v. 5, No. 3, Sept. 1958, pp. 217 – 221.

[40] B. Mann, G. Heydt, "Non-collocated voltage and current measurements used to obtain power," submitted for publication, Letters, IEEE Transactions on Power Systems, 2006.

[41] B.Mann, G. Heydt, "Non-collocated power measurements in a power system state estimator," North American Power Symposium, Oct. 23-25, 2005.

APPENDIX A

DESCRIPTION OF THE TEST CASES

Table A.1 Guide to the test case denomination and meaning

Case	Description	Test bed	Random measurement error	Results at
A	Solution method for non-collocated measurements with the reference voltage available	-	-	-
B	Solution method for non-collocated measurements with non-reference voltage available	-	-	-
0	Base case state estimation	11-bus	None	Tables 2.4-2.8
1	State estimation with noise	11-bus	10%	Tables 2.4-2.8
2	State estimation with noise	11-bus	30%	Tables 2.4-2.8
3	State estimation with noise and a non-collocated measurement	11-bus	10%	Tables 2.4-2.8
4	State estimation with noise and a non-collocated measurement	11-bus	30%	Tables 2.4-2.8
5	Unbalanced state estimation with single-phase measurements	3-bus	*a* – none, *b* – 10%	Tables 3.6-3.7
6	Unbalanced state estimation with single-phase measurements and correction factor	3-bus	*a* – none, *b* – 10%	Tables 3.6-3.7
7	Unbalanced state estimation with three-phase measurements	3-bus	*a* – none, *b* – 10%	Tables 3.6-3.7
8	Unbalanced state estimation with three-phase measurements with correction factor	3-bus	*a* – none, *b* – 10%	Tables 3.6-3.7
9	Measurement prediction algorithm with *A* matrix calculated once with latency and low bandwidth	5-bus	*a* – none, *b* – 10%	Table 4.2
10	Measurement prediction algorithm with *A* matrix calculated once without latency and low bandwidth	5-bus	*a* – none, *b* – 10%	Table 4.2
11	Measurement prediction algorithm with *A* matrix updated continuously and low bandwidth	5-bus	*a* – none, *b* – 10%	Table 4.2
12	Measurement prediction algorithm with *A* matrix calculated once with latency and high bandwidth	5-bus	*a* – none, *b* – 10%	Table 4.2
13	Measurement prediction algorithm with *A* matrix calculated once without latency and high bandwidth	5-bus	*a* – none, *b* – 10%	Table 4.2
14	Measurement prediction algorithm with *A* matrix updated continuously and high bandwidth	5-bus	*a* – none, *b* – 10%	Table 4.2

APPENDIX B

SAMPLE MATLAB CODE

Presented here is the Matlab code used in generating the Test Case 0.4 results used in Chapter 2.

```
% Non-collocated measurement state-estimation
clear;

format long

%reactance calculation, from rough line length data and exact conductor
%spacing data.
%Line type 1, Bluebird, 2-bundled d=18inches, D=25ft, flat spacing
smalld=(18/12)/3.28;
bigd=25/3.28;
gmr=.0588/3.28;
dsl=sqrt(gmr*smalld);
deq=(bigd*bigd*(2*bigd))^(1/3);
% Units here are H/m
la=(2e-7)*log(deq/dsl);
la=la*1000;
la=la/.6213712;
%Here we have reactance per mile, divided by the X base into per unit
base=((500e3)^2)/(100e6);
xa=(2*pi*60*la)/base;

a=150*xa;
a=(a*a)/(a+a);
b=17.65*xa;
e=55.17*xa;
e=(e*e)/(e+e);
f=213.55*xa;
%accounting for the capacitors at Bus 2 (Imperial valley)
j=(62.5*xa)-.01022;
k=87.5*xa-.00995;
l=68.75*xa;

%Line type 2, Cardinal, 3-bundled d=18inches, D=25ft, flat spacing
gmr=.0403/3.28;
dsl=(gmr*(smalld)^2)^(1/3);
la=(2e-7)*log(deq/dsl);
la=la*1000;
la=la/.6213712;
xa=(2*pi*60*la)/base;

c=162.5*xa;
d=7.5*xa;
g=62.5*xa;
g=(g*g)/(g+g);
h=100*xa;

%Correct angles - bus 11 is the ref bus and is exactly delta=0.0000
dl=[.05;.07;.08;.10;.08;0;-.01;-.03;-.02;-.01;0];
%Correct bus voltage magnitudes
vbus=[1;1.01;1.02;1.00;1.02;1;.98;.97;1;1.03;1.03];
%Correct complex bus voltage
```

```
vm=vbus.*(cos(dl)+i*sin(dl));
%Get diff in bus voltages
li=[vm(2)-vm(1);vm(3)-vm(2);vm(4)-vm(3);vm(4)-vm(5);vm(4)-vm(6);...
        vm(4)-vm(11);vm(6)-vm(7); vm(7)-vm(8);vm(9)-vm(8);vm(10)-
vm(9);...
        vm(11)-vm(10)];
%Line currents
li=li./(i*[j;k;l;h;g;f;d;c;b;a;e]);
%Real part of line complex powers
mm=real([vm(2)*li(1)';vm(3)*li(2)';vm(4)*li(3)';vm(4)*li(4)';...
        vm(4)*li(5)';vm(4)*li(6)';vm(6)*li(5)';vm(6)*li(7)';...
        vm(7)*li(7)';vm(8)*li(8)';vm(9)*li(9)';vm(10)*li(10)';...
        vm(10)*li(11)';vm(11)*li(6)';vm(11)*li(6)'-vm(11)*li(11)';...
        vm(4)*(li(4)'+li(5)'+li(6)'+li(3)'); vm(9)*(li(10)'-li(9)');...
        vm(6)*(li(5)'-li(7)')]);
%Reactive part of line complex powers
mmq=imag([vm(2)*li(1)';vm(3)*li(2)';vm(4)*li(3)';vm(4)*li(4)';...
        vm(4)*li(5)';vm(4)*li(6)';vm(6)*li(5)';vm(6)*li(7)';...
        vm(7)*li(7)';vm(8)*li(8)';vm(9)*li(9)';vm(10)*li(10)';...
        vm(10)*li(11)';vm(11)*li(6)';vm(11)*li(6)'-vm(11)*li(11)';...
        vm(4)*(li(4)'+li(5)'+li(6)'+li(3)'); vm(9)*(li(10)'-li(9)');...
        vm(6)*(li(5)'-li(7)')]);

%Process matrix H from SE calculation z=Hx
hh=zeros(18,11);
hh(1,2)=1/j;
hh(1,1)=-hh(1,2);
hh(2,3)=1/k;
hh(2,2)=-hh(2,3);
hh(3,4)=1/l;
hh(3,3)=-hh(3,4);
hh(4,4)=1/h;
hh(4,5)=-hh(4,4);
hh(5,4)=1/g;
hh(5,6)=-hh(5,4);
hh(6,4)=1/f;
hh(6,11)=-hh(6,4);
hh(7,4)=1/g;
hh(7,6)=-hh(7,4);
hh(8,6)=1/d;
hh(8,7)=-hh(8,6);
hh(9,6)=1/d;
hh(9,7)=-hh(9,6);
hh(10,7)=1/c;
hh(10,8)=-hh(10,7);
hh(11,9)=1/b;
hh(11,8)=-hh(11,9);
hh(12,10)=1/a;
hh(12,9)=-hh(12,10);
hh(13,11)=1/e;
hh(13,10)=-hh(13,11);
hh(14,4)=1/f;
hh(14,11)=-hh(14,4);
hh(15,4)=1/f;
hh(15,10)=1/e;
hh(15,11)=-hh(15,4)-hh(15, 10);
hh(16,5)=-1/h;
```

```
hh(16,3)=-1/l;
hh(16,11)=-1/f;
hh(16,6)=-1/g;
hh(16,4)=-hh(16,5)-hh(16,11)-hh(16,3)-hh(16,6);
hh(17,10)=1/a;
hh(17,8)=1/b;
hh(17,9)=-hh(17,10)-hh(17,8);
hh(18,4)=1/g;
hh(18,7)=1/d;
hh(18,6)=-hh(18,4)-hh(18,7);

% Here, mmnc are matricies of power measurements that contain a
%   a non-collocated measurement at M1
% mmnc2 is for V1I2* non-collocation, mmnc2 is for V2I1*
%   non-collocation
vee1=vm(2)+(li(2)*i*-.00995);
eye1=li(2);
eye2=li(1);
vee2=vm(2)-eye2*j*-.01022;
mmnc1=mm;
mmnc2=mm;
mmnc1(1)=real(vee2*eye1');
mmnc2(1)=real(vee1*eye2');
mmnc1q=mmq;
mmnc2q=mmq;
mmnc1q(1)=imag(vee2*eye1');
mmnc2q(1)=imag(vee1*eye2');

%At this point, estimate deltas using correct power measurements
deltahat=pinv(hh(1:18,1:10))*mm;
deltahat(11)=0;

veehat=pinv(hh(1:18,1:10))*mmq;
%Fill veehat in position 11 with correct value to get proper norms
veehat(11)=vbus(11)-1;

%Here are a series of variable declarations
peeps=0;
tenpmm=mm;
tenpmmq=mmq;
tenpave=0;
tenpexave=0;
tenpexaveq=0;
tenpresidualave=0;
tenpresidualaveq=0;

thirtypmm=mm;
thirtypmmq=mmq;
thirtypexave=0;
thirtypexaveq=0;
thirtypresidualave=0;
thirtypresidualaveq=0;

tenpmmnc=mmnc1;
tenpmmncq=mmnc1q;
tenpexavenc=0;
```

```
tenpexavencq=0;
tenpresidualavenc=0;
tenpresidualavencq=0;

thirtypmmnc=mmnc1;
thirtypmmncq=mmnc1q;
thirtypexavenc=0;
thirtypexavencq=0;
thirtypresidualavenc=0;
thirtypresidualavencq=0;

%Peeps is simply a counter variable
for peeps=1:1000
    tenpmm=mm;
    tenpmmq=mmq;
    thirtypmm=mm;
    thirtypmmq=mmq;
    tenpmmnc=mmnc1;
    tenpmmncq=mmnc1q;
    thirtypmmnc=mmnc1;
    thirtypmmncq=mmnc1q;
    %In this next loop, percent error is introduced
    %   There are 10% and 30% measurement error cases
    %   the variables with 'mm' contain no non-collocation
    %   whereas variables with mmnc contain non-collocation
    for pops=1:18
        tenpmm(pops)=tenpmm(pops)+((tenpmm(pops)*2*rand(1)/10)-
tenpmm(pops)/10);
        tenpmmq(pops)=tenpmmq(pops)+((tenpmmq(pops)*2*rand(1)/10)-
tenpmmq(pops)/10);

thirtypmm(pops)=thirtypmm(pops)+((thirtypmm(pops)*2*3*rand(1)/10)-
3*thirtypmm(pops)/10);

thirtypmmq(pops)=thirtypmmq(pops)+((thirtypmmq(pops)*2*3*rand(1)/10)-
3*thirtypmmq(pops)/10);
        tenpmmnc(pops)=tenpmmnc(pops)+((tenpmmnc(pops)*2*rand(1)/10)-
tenpmmnc(pops)/10);

tenpmmncq(pops)=tenpmmncq(pops)+((tenpmmncq(pops)*2*rand(1)/10)-
tenpmmncq(pops)/10);

thirtypmmnc(pops)=thirtypmmnc(pops)+((thirtypmmnc(pops)*2*3*rand(1)/10)
-3*thirtypmmnc(pops)/10);

thirtypmmncq(pops)=thirtypmmncq(pops)+((thirtypmmncq(pops)*2*3*rand(1)/
10)-3*thirtypmmncq(pops)/10);
    end
    % Here is the state estimation for bus angle and voltage magnitude
    tenpdeltahat=pinv(hh)*tenpmm;
    tenpveehat=pinv(hh)*tenpmmq;

    % Here the residual is taken between the SE results and the actual
    % results for all of the test cases
    tenpexave=tenpexave+(deltahat-tenpdeltahat);
    tenpexaveq=tenpexaveq+(veehat-tenpveehat);
```

```
    tenpresidualave=tenpresidualave+(hh*tenpdeltahat-mm);
    tenpresidualaveq=tenpresidualaveq+(hh*tenpveehat-mmq);

    thirtypdeltahat=pinv(hh)*thirtypmm;
    thirtypveehat=pinv(hh)*thirtypmmq;
    thirtypexave=thirtypexave+(deltahat-thirtypdeltahat);
    thirtypexaveq=thirtypexaveq+(veehat-thirtypveehat);
    thirtypresidualave=thirtypresidualave+(hh*thirtypdeltahat-mm);
    thirtypresidualaveq=thirtypresidualaveq+(hh*thirtypveehat-mmq);

    tenpdeltahatnc=pinv(hh)*tenpmmnc;
    tenpveehatnc=pinv(hh)*tenpmmncq;
    tenpexavenc=tenpexavenc+(deltahat-tenpdeltahatnc);
    tenpexavencq=tenpexavencq+(veehat-tenpveehatnc);
    tenpresidualavenc=tenpresidualavenc+(hh*tenpdeltahatnc-mm);
    tenpresidualavencq=tenpresidualavencq+(hh*tenpveehatnc-mmq);

    thirtypdeltahatnc=pinv(hh)*thirtypmmnc;
    thirtypveehatnc=pinv(hh)*thirtypmmncq;
    thirtypexavenc=thirtypexavenc+(deltahat-thirtypdeltahatnc);
    thirtypexavencq=thirtypexavencq+(veehat-thirtypveehatnc);
    thirtypresidualavenc=thirtypresidualavenc+(hh*thirtypdeltahatnc-
mm);
    thirtypresidualavencq=thirtypresidualavencq+(hh*thirtypveehatnc-
mmq);


end

%Next, the average of the 1000 state estimation resuslts for each test
Case
%   is calculated. Then, the norms of the residual (z_hat-z)
%   is taken.
tenpexave=tenpexave/1000;
tenpresidualave=tenpresidualave/1000;
tenp_ex_norm=norm(tenpexave);
tenp_residual_norm=norm(tenpresidualave);
tenp_ex_mean=mean(tenpexave);

tenpexaveq=tenpexaveq/1000;
tenpresidualaveq=tenpresidualaveq/1000;
tenp_ex_norm_q=norm(tenpexaveq);
tenp_residual_norm_q=norm(tenpresidualaveq);
tenp_ex_meanq=mean(tenpexaveq);

thirtypexave=thirtypexave/1000;
thirtypresidualave=thirtypresidualave/1000;
thirtyp_ex_norm=norm(thirtypexave);
thirtyp_residual_norm=norm(thirtypresidualave);
thirtyp_en_mean=mean(thirtypexave);

thirtypexaveq=thirtypexaveq/1000;
thirtypresidualaveq=thirtypresidualaveq/1000;
thirtyp_ex_norm_q=norm(thirtypexaveq);
thirtyp_residual_norm_q=norm(thirtypresidualaveq);
```

```
tenpexavenc=tenpexavenc/1000;
tenpresidualavenc=tenpresidualavenc/1000;
tenp_ex_norm_nc=norm(tenpexavenc);
tenp_residual_norm_nc=norm(tenpresidualavenc);

tenpexavencq=tenpexavencq/1000;
tenpresidualavencq=tenpresidualavencq/1000;
tenp_ex_norm_nc_q=norm(tenpexavencq);
tenp_residual_norm_nc_q=norm(tenpresidualavencq);

thirtypexavenc=thirtypexavenc/1000;
thirtypresidualavenc=thirtypresidualavenc/1000;
thirtyp_ex_norm_nc=norm(thirtypexavenc);
thirtyp_residual_norm_nc=norm(thirtypresidualavenc);

thirtypexavencq=thirtypexavencq/1000;
thirtypresidualavencq=thirtypresidualavencq/1000;
thirtyp_ex_norm_nc_q=norm(thirtypexavencq);
thirtyp_residual_norm_nc_q=norm(thirtypresidualavencq);
```

The next three Matlab programs represent the Test Case 12a conducted in Chapter 4.

```
% Delayed measurerment state estimation program, delayse.m
% This program creates data for a 5 bus, seven
%   measurement power system. The state estimation
%   will be for bus voltage angles with real power
%   measurements.
% This program is for the high-bandwidth, noisless
%   case where A is claculated once. This is test
%   Case 12a, also explained in Appendix A and
%   Table 4.1. results are shown in Table 4.2.

clear;
format long;

%mem is the number of previous measurements to be
%   kept in memory, known as n+1 in the thesis.
mem=5;

% The delayb program creates a set of non-periodic
%   arbitrarily chosen set of 7 measurements.
%   The real measurements are in the matrix "meas."
%   The program delay also randomly delays some
%   of these measurements by one time period
%   (there is a 5% chance of any measurement being
%   delayed). The delayed measurements are in matrix
%   "dmeas." The time period is from time 0 to 10
%   in .05 second intervals. The code for delayb
%   is included.

delayb

% Here the real, non-delayed data is put into the
%   state estimator. This will be compared to the
%   delayed case and the fixed delayed case later.

%Here the H matrix is defined, such that z=Hx
% for the 5 bus, 7 measurement system
H=zeros(7,5);
H(1,1)=-inv(.05);
H(1,3)=inv(.05);
H(2,1)=-inv(.01);
H(2,2)=inv(.01);
H(3,2)=-inv(.01);
H(3,3)=inv(.01);
H(4,1)=-inv(.05);
H(4,2)=-inv(.01);
H(4,3)=inv(.05)+inv(.01)+inv(.02);
H(4,4)=-inv(.02);
H(5,3)=inv(.02);
H(5,4)=-inv(.02);
H(6,3)=inv(.02);
H(6,4)=-inv(.02);
H(7,4)=inv(.03);
H(7,5)=-inv(.03);
```

```
% States are calculated from the real
%   and delayed measurements.
for i=1:length(time)+1
    % For the real measurements
    statereal(:,i)=pinv(H)*meas(:,i);
    % For the randomly relayed measurements
    statedelay(:,i)=pinv(H)*dmeas(:,i);
end

%And here is the correction algorithm. The Matrix A
%   is calculated once. Code for this is also included.

corrections

for i=1:length(time)+1
    % For the corrected measurements from algorithm corrections
    statereal(:,i)=pinv(H)*peas(:,i);
end

% It was useful to place graph plotting commands here
```

```
% Delayed measurement test bed, delayb.m

% the discrete time period for this study
% original delta: .05
delta=.05;
time=[0:delta:10];
time1=[0:delta:10+delta];

% Here none-repeating sinusoids are used to generate a measurement sig-
nal
meas=zeros(7,length(time));
for i=1:length(time)+1;

meas(1,i)=sin(.1*i*delta)+2*sin(.1*sqrt(2)*i*delta)+3*sin(.1*sqrt(3)*i*
delta);

meas(2,i)=sin(.1*sqrt(3)*i*delta)+2*sin(.1*i*delta)+3*cos(.1*sqrt(3)*i*
delta);
    meas(3,i)=cos(.1*i*delta)+sqrt(3)*sin(.1*sqrt(2)*i*delta);
    meas(5,i)=2*cos(.1*i*delta)+cos(.1*sqrt(3)*i*delta);
    meas(4,i)=meas(3,i)-meas(5,i)+meas(1,i);
    meas(6,i)=meas(5,i);
    meas(7,i)=2*sin(.1*sqrt(2)*i*delta)+sqrt(3)*cos(.1*i*delta);
end

% Here the noiseless measurements are randomly delayed
dmeas(:,1)=meas(:,1);
for i=2:length(time)+1
    for j=1:7
        if rand(1)<=.05
            dmeas(j,i)=meas(j,i-1);
        else
            dmeas(j,i)=meas(j,i);
        end
    end
end
```

```
% The measurement correction algorithm, corrections.m

correction=0;
delayedmeas=0;
same=0;

% pmeas will ultimately hold the corrected measurements
pmeas(:,1:11)=dmeas(:,1:11);

% These variables insure that measurement replacement
%   will not occur for mem sampling periods after
%   a successful measurement replacement
countdown=zeros(7,1);
subcountdown=zeros(7,1);

% Here the matrix A from the algorithm is calculated
prev(:,1:mem)=dmeas(:,1:mem);
prev(:,mem+1)=dmeas(:,mem+1);
A=pinv(prev(:,1:mem))*prev(:,(mem+1));


for t=(mem+2):length(time)+1

    % Here the predicition is made (ppredict) and put into a matrix
    %   of all proposed corrections: predict.
    prev(:,1:mem)=dmeas(:,t-(mem+1):t-2);
    prev(:,mem+1)=dmeas(:,t-1);
    ppredict=dmeas(:,t-mem:t-1)*A;
    predict(:,t)=ppredict;


    for m=1:7

        % 0.001 is the sorting factor. If the predicition differs from
        %   the measurement by more then this, it may be replaced if
        %   there has been no replacement in the past mem sampling
        %   periods.
        if abs(ppredict(m)-dmeas(m,t))<=.001 || countdown(m)>0
            pmeas(m,t)=dmeas(m,t);
        else
           pmeas(m,t)=ppredict(m);
           subcountdown(m)=1;
        end

        % It was useful to keep track of how often the replaced
        %   measurement was closer to the actual measurement than
        %   the randomly delayed measurements. Here is the code
        %   for that.
        if abs(pmeas(m,t)-meas(m,t))<abs(dmeas(m,t)-meas(m,t))
            correction=correction+1;
        elseif abs(pmeas(m,t)-meas(m,t))==abs(dmeas(m,t)-meas(m,t))
            same=same+1;
        else
            delayedmeas=delayedmeas+1;
        end
```

```
    end
    % This next loop manages the countdown to insure measurements
    %   will not be corrected more than once during mem sampling
    %   periods
    for m=1:7
        if subcountdown(m)==1 && countdown(m)==0
            countdown(m)=mem+1;
            subcountdown(m)=0;
        elseif subcountdown(m)==1 && countdown(m)~=0
            subcountdown(m)=0;
        end
        if countdown(m)>0
            countdown(m)=countdown(m)-1;
        end
    end
end
% Now the number of better outcomes for the delayed and corrected sig-
nal
%   shown, and also the 2-norm residuals of the measurement residuals.
correction
delayedmeas
same
corrected=norm(pmeas-meas)
uncorrected=norm(dmeas-meas)
```